SILICA DISSOLUTION FROM OIL SANDS

By: J. Boon

Geochemistry Group

Oil Sands Research Centre

August, 1979

TABLE OF CONTENTS

PAGE

SUMMARY AND CONCLUSIONS

Published literature on silica solubility, dissolution rates and precipitation rate is reviewed. The dissolution rate of SiO_2 from quartz and oil sand samples was determined as a function of temperature, pH, solid:liquid ratio and presence or absence of bitumen. A number of amorphous silica and quartz precipitation experiments were carried out at different temperatures, in both static and agitated solutions. The surface of the solids remaining after the dissolution experiments was studied with the scanning electron microscope. The dissolution rate constants that were obtained from the experimental work were used to model SiO_2 dissolution in the ARC 150 cm physical simulator and SiO_2 precipitation in a hypothetical field case.

CONCLUSIONS

1. Up to pH 7.5, the activation energy for dissolution of SiO_2 from oil sand is 14.4 ± 1.4 kcal $mole^{-1}$ and pH does not influence the dissolution rate. At pH 8.7 it is in the range of 25 - 27 kcal $mole^{-1}$ and the dissolution rate is much greater, as are the equilibrium concentrations.

2. Bitumen lowers the SiO_2 dissolution rate, probably by physical surface coverage.

3. Two dissolution processes are occurring, one of which is virtually complete during the initial stages of the experiments. The extent to which the rapid initial process occurs depends on the sample history and varies throughout a bulk sand sample.

4. At high pH, analcime crystals grow on the surface of the quartz grains, in some cases in large enough quantity to close off pore throats and affect permeability.

5. At high pH, the surface area of the sand strongly decreases during reaction, probably because part of the < 45 μm fraction dissolves completely.

6. At pH ≤ 7.5, and solid to liquid ratios ≤ 66.7 g l^{-1}, diffusion of dissolved SiO_2 out of the intergranular pore system into the bulk liquid phase (in static experiments) is faster than reaction at the surface. At pH 8.7, diffusion of SiO_2 out of the intergranular pore space is the rate-determining step at solid:liquid ratios > 2.5 g l^{-1} (at 200°C) or > 1.0 g l^{-1} (at 250°C).

7. The precipitation of amorphous silica involves an induction period (nucleation step). Quartz does not provide nucleation sites. Nucleation is facilitated at higher temperatures. The aluminum liberated from the clay minerals in the oil sand counteract the catalytic action of fluoride ions. Reaction times to equilibrium are short.

8. The precipitation of quartz is strongly influenced by the experimental set up: the precipitation rate is much faster in rocking bomb experiments than in static bomb experiments. In the former experiments, the SiO_2 concentration decreased to values well below quartz saturation on a number of occasions. An explanation has yet to be put forth.

9. Numerical methods are needed to accurately predict SiO_2 concentrations and dissolution rates in the 150 cm physical simulator or in a field situation.

10. Steady state approximations correctly predicted that the production fluids from the 150 cm physical simulator will be undersaturated with respect to quartz, but did not agree with the measured value. Dissolution rates in the 150 cm physical

simulator can be of the order of 1 to 4% by weight of the rock matrix per 100 hours. Precipitation rates in a field case can reach up to 8% by weight of the rock matrix per 417 days.

LIST OF TABLES

LIST OF FIGURES AND PLATES

PAGE

INTRODUCTION

The major mineral component of the Alberta Oil Sands deposits (excluding those in carbonate rocks) is quartz that occurs either in coarse or in microcrystalline form (chert). Most in situ processes being proposed for the recovery of bitumen involve the injection of large volumes of water and steam into the formation. The dissolution of SiO_2 in the high temperature regions of the production zone and its subsequent precipitation in cooler parts of the formation could lead to a significant decrease of permeability. This reaction is suspected to have been the cause of large pressure drops in the Shell and Petro Fina field experiments (REDFORD and COTSWORTH, 1974).

Cementation and formation of overgrowths as a result of the precipitation of silica from the interstitial solutions are common causes for porosity and permeability reductions during diagenesis (PETTIJOHN, POTTER and SIEVER, 1972). This has also been demonstrated experimentally (CECIL and HEALD, 1971; ERNST and BLATT, 1964; HEALD and RENTON, 1966; PARAGUASSA, 1972; SPRUNT and NUR, 1976). However, the geological literature on diagenesis is of little help in predicting the behavior of silica during steam injection because the time scales involved are altogether different. Most of the experimental work on cementation reported in the literature was carried out at pressures of 100 MPa or higher, and temperatures up to 400°C, whereas during the injection of steam into the oil sands the maximum temperatures that will be reached are in the range around 300°C at the corresponding saturated water vapour pressure (8.58 MPa). During in situ combustion the temperature can rise as high as 600°C, but the pressure will remain well below 100 MPa.

Dissolved silica also takes part in reactions such as: H_4SiO_4 + kaolinite + calcite $\rightleftarrows$ montmorillonite + H_2CO_3 (BAYLISS and LEVINSON, 1971).

The degree to which formation porosity and permeability are affected by the dissolution and precipitation of silica depends to a large extent on the kinetics of these reactions. Also, the dissolution of quartz can be the rate-determining step in mineral formation reactions, as was shown by COURNOYER et al. (1975) for the formation of zeolite from an aluminate solution that was in contact with solid quartz.

To complement other studies in this laboratory an experimental study of the dissolution and precipitation rates of quartz in the oil sand-water system was carried out. The present report describes and interprets the results of dissolution rate experiments conducted at pH levels between 5.6 and 8.7 and at temperatures ranging from 150°C to 250°C, both in the presence and in the absence of bitumen. Attention is paid to the way in which the experimental set-up has influenced the results, in particular with respect to the fraction of the sand surface that actually takes part in the dissolution process. Product minerals that formed during some of the dissolution experiments are described and identified with the aid of scanning electron micrographs and X-ray diffraction. Also, the results of some preliminary precipitation rate experiments are discussed. In a final section of the report the steady state SiO_2 concentration and dissolution rate in the ARC-AOSTRA 150 cm physical simulator are calculated as a function of distance from the injector, using the rate equations derived in the earlier sections. Steady state concentrations and SiO_2 precipitation rates are calculated for a hypothetical field case.

LITERATURE REPORTS

Silica occurs in many forms, only two of which are of immediate interest: low quartz, the mineral that occurs in the oil sands, and amorphous silica, that may precipitate from highly supersaturated silica solutions. So far, no occurrences of amorphous silica in undisturbed oil sands have been reported.

SOLUBILITY

WALTHER AND HELGESON (1977) provided a comprehensive survey of the published literature on the solubility of the various silica polymorphs. They derived an equation of state for aqueous silica and computed the solubility of each of the polymorphs as a function of temperature at pressures corresponding to the liquid vapor equilibrium curve for H_2O. The data in Table 1 were calculated from those in WALTHER and HELGESON'S (1977) Table 2.

CRERAR and ANDERSON (1971) derived the following regression equation for the solubility of quartz from published data and from their own solubility measurements:

$$\log (\text{ppm } SiO_2) = a + bx_i + cx_i^2 \qquad (1)$$

where:

$x_i = 1000/T \quad K^{-1}$

and:

$a = 3.3105$

$b = 0.25293$

$c = -0.32168$

Solubility values obtained in this laboratory agreed more closely with those calculated from equation (1) than with those calculated by WALTHER and HELGESON (1977). Their calculated solubilities for amorphous silica agree reasonably well with literature values, whereas those for quartz are somewhat lower than published values in the 200°C - 300°C range.

All solubility data cited above refer to the system SiO_2 - H_2O. The dissolution reaction can be formally represented by:

$$SiO_2(s) + 2H_2O \rightleftarrows H_4SiO_4 \qquad (2)$$

Table 1. The equilibrium concentration of SiO_2 (mg kg^{-1}) for various silica polymorphs at pressures and temperatures corresponding to the liquid-vapor equilibrium curve for H_2O. Calculated from WALTHER and HELGESON'S (1977), Table 2, assuming that the density of the solution equals that of pure water at the same pressure and temperature.

T (°C)	P (MPa)	α-Quartz	α-Cristobalite	"β-Cristobalite"	Chalcedony	Amorphous Silica
0.	0.10	2.	8.	26.	4.	61.
5.	0.10	2.	10.	31.	5.	71.
10.	0.10	3.	12.	37.	6.	81.
25.	0.10	6.	21.	59.	11.	116.
50.	0.10	14.	45.	109.	25.	187.
75.	0.10	29.	79.	173.	49.	275.
100.	0.10	48.	127.	253.	80.	378.
125.	0.23	77.	187.	349.	123.	498.
150.	0.49	115.	262.	460.	178.	632.
175.	0.89	164.	353.	587.	247.	778.
200.	1.55	225.	459.	729.	330.	935.
225.	2.55	298.	581.	887.	427.	1093.
250.	3.97	384.	717.	1059.	537.	1253.
275.	5.94	482.	865.	1241.	657.	1396.
300.	8.59	586.	1013.	1413.	779.	1516.
325.	12.04	685.	1145.	1573.	887.	1581.
350.	16.51	741.	1199.	1617.	931.	1527.

with the equilibrium constant

$$K = a_{H_4SiO_4}/a_{H_2O} \tag{3}$$

H_4SiO_4 dissociates according to the reaction

$$H_4SiO_4 \overset{\leftarrow}{\rightarrow} H^+ + H_3SiO_4^- \tag{4}$$

which has an equilibrium constant

$$K_1 = \frac{a_{H^+}\, a_{H_3SiO_4^-}}{a_{H_4SiO_4}} \tag{5}$$

Consequently, the total amount of silica in solution increases with increasing pH. SEWARD (1974) determined K_1 for temperatures up to 350°C and found that dissociation is negligible below pH 8.0. He also noted that, in Na^+ - containing solutions, ion pairing may occur:

$$H_3SiO_4^- + Na^+ \overset{\leftarrow}{\rightarrow} NaH_3SiO_4^0$$

$$K_{as} = \frac{a_{NaH_3SiO_4}}{a_{H_3SiO_4^-}\, a_{Na^+}} \tag{7}$$

SEWARD used borate buffer solutions and calculated the pH of these at elevated temperatures. The assumptions on which he based his calculations have been questioned recently and the real pH in his experiments may have been much higher than the calculated value (J. D. RIMSTIDT, personal communication). Consequently, SEWARD may have overestimated the importance of $Na^+ - H_3SiO_4^-$ ion pairing.

Unless indicated otherwise, all SiO_2 concentrations are expressed in mg l^{-1} at room temperature.

DISSOLUTION RATES

According to VAN LIER et al (1960) and COURNOYER et al (1975) the dissolution of quartz is reaction-controlled and the forward rate of reaction (2) is described by the equation:

$$\left(\frac{dc}{dt}\right)_f = k_1 \frac{S}{V} \tag{8}$$

where:

k_1 = forward rate constant

S = surface area

V = liquid volume

At equilibrium, the backward rate equals the forward rate and

$$K = \frac{k_1}{k_2} \tag{9}$$

where:

k_2 = backward rate constant

Assuming that $a_{H_2O} = 1$ and $a_{H_4SiO_4} = C_{H_4SiO_4}$, combination of (3), (8) and (9) yields the backward rate of reaction:

$$\left(\frac{dc}{dt}\right)_b = -k_2 C \frac{S}{V} = -k_1 \frac{C\ S}{K\ V} \tag{10}$$

The net rate of concentration change is given by

$$\frac{dc}{dt} = \left(\frac{dc}{dt}\right)_f + \left(\frac{dc}{dt}\right)_b = \frac{k_1 S}{V} \left(1 - \frac{C}{K}\right) \tag{11}$$

or

$$\frac{dc}{dt} = \frac{k_1 S}{V} \left(1 - \frac{C}{C_{eq}}\right) \tag{12}$$

where:

C_{eq} = the equilibrium concentration of SiO_2.

For the case in which a quartz porous medium reacts with the pore fluid, (12) takes the form

$$\frac{dc}{dt} = \frac{k_1 \rho A'}{\Phi} (1 - C/C_{eq}) \tag{13}$$

where:

ρ = bulk density of the dry porous medium

A' = surface area per unit weight of dry porous medium

Φ = porosity

Integration of equation (12) yields:

$$\ln \left(\frac{C_{eq} - C}{C_{eq} - C_0} \right) = \frac{k_1 S}{C_{eq} V} t \tag{14}$$

where:

C_0 = SiO_2 concentration at $t = 0$

The temperature dependence of the rate constant can be described by the Arrhenius relation:

$$k_1 = k_1' \exp (-E_a/RT) \tag{15}$$

where:

k_1' = constant

E_a = activation energy for dissolution

R = gas constant

VAN LIER et al (1960) reported k_1 = 3.16 x 10^{-15}g SiO_2 cm^{-2} sec^{-1} = 1.138 x 10^{-5} µg SiO_2 cm^{-2} hr^{-1} at 70°C. COURNOYER et at (1975) found a value of 21.7 kcal $mole^{-1}$ for the activation energy for dissolution of quartz in alkaline solutions between 64°C and 123°C. No literature reports on dissolution rates at higher temperatures were available when the present investigation was started. Recently, RIMSTIDT and BARNES (1977) reported an activation energy of 19.2 kcal $mole^{-1}$ in distilled water. According to VAN LIER et al (1960), k_1 for quartz is influenced by temperature, pH and the presence of NaCl. DOREMUS and ALIM-MARVASTI (1973) drew similar conclusions for amorphous silica.

Various authors reported that the grinding of quartz produces a disturbed surface layer of high solubility (BERGMAN, 1963; HENDERSON et al, 1970; VAN LIER et al; 1960). They assumed that this layer was responsible for the rapid initial dissolution stage they observed in their experiments. MOORE and ROSE (1975), however, found no evidence for the presence of such a layer and they explained the rapid initial dissolution by the adherence of very fine particles to large grains or by the formation of a hydrated surface layer during grinding. DOREMUS and ALIM-MARVASTI (1973) observed a similar dissolution behavior for amorphous silica that had not been ground prior to the experiment. These authors also noted that the dissolution of amorphous silica is reaction-controlled.

PRECIPITATION RATE

OWEN (1975) reviewed the literature on polymerization and precipitation of amorphous silica. From that review and later work (HARVEY et al, 1976; BOON, 1977a) the following conclusions can be drawn:

1. Monomeric silica (H_4SiO_4) is the primary aqueous silica species in solutions saturated with respect to amorphous silica at pH less than 8.0.

2. The polymerization rate of silica increases with temperature and with the degree of supersaturation. At supersaturations (C/C_{eq}) less than 3 an induction time is observed. Seeding with amorphous silica leads to immediate precipitation. The activation energy for polymerization is 9.8 kcal $mole^{-1}$ (KITAHARA, 1960).

3. The polymerization rate constant has a maximum at pH = 7.5. At lower pH the polymerization reaction is second order, at higher pH it is third order. An increase in pH leads to a decreased induction period.

4. High salt concentrations decrease the solubility of amorphous silica and thereby increase the nucleation rate.

No published values for the precipitation rate of quartz were available when the present study was started. RIMSTIDT and BARNES (1977) reported an activation energy for quartz precipitation of 12 kcal $mole^{-1}$. Further details of their work are described in a paper that has been submitted to Geochimica et Cosmochimica Acta. According to these authors, equation (13) applies to the precipitation of quartz during flow through a quartz sand core.

Various authors observed the formation of quartz overgrowths when sand or sandstone reacted with aqueous fluids at high temperatures and pressures (ERNST and BLATT, 1964; MAXWELL, 1960). HEALD and RENTON (1966) placed the autoclaves in a thermal gradient and found that the precipitation of quartz at the cooler end caused a significant porosity reduction. Fine sand grains grew faster than coarse sand grains and monocrystalline grains grew faster than polycrystalline grains. CECIL and HEALD (1971) observed that, under similar experimental conditions, the formation of secondary quartz was prevented by the presence of iron oxide, calcium carbonate or clay coatings on the sand grains. The experiments were conducted at temperatures between 255°C and 300°C. The temperature difference

between the hot and cold zones was 70°C and pressures ranged from 13.79 MPa to 75.84 MPa. The duration of the experiments varied between 8 and 114 hours and weakly alkaline (0.03 M Na_2CO_3) to strongly alkaline (0.25 M NaOH) solutions were used.

From the literature results that were reviewed above, it can be concluded that both amorphous silica and quartz precipitation may occur to a significant extent during in situ recovery of bitumen by wet thermal methods. For example, if the temperature of the injected steam is 250°C and the travel time from the injector to producer is long enough to achieve saturation, the condensed fluids will contain 415 mg l^{-1} of silica by the time they reach the production well. Pressure release of the condensed fluid to atmospheric pressure near the production well bore produces 30% quality steam at 100°C and the silica concentration in the condensed aqueous phase thereby increases to 593 mg l^{-1}. The amorphous silica saturation concentration at this temperature is 378 mg l^{-1} and, depending on the pH, precipitation of amorphous silica could well take place close to or inside the well bore, leading to formation damage and/or malfunctioning of downhole equipment. The latter problem occurred during pilot tests carried out by one of the major oil companies (GEWERS, Esso Resources, personal communication). Downhole acidification of production fluids may be a possible remedy, however, the economics, technical problems and the possible side effects (corrosion, breaking of emulsions) of such a treatment would have to be taken into account. The alkalinity of the steam condensate is much less than that of the various solutions used by HEALD and RENTON (1966) but the residence time of the fluids in the formation is much longer; quartz therefore will precipitate within the formation in regions where a temperature gradient occurs. The magnitude of the permeability change caused by quartz or amorphous silica precipitation is controlled by the combined effects of flow rate and precipitation rate. The latter depends on temperature, pH and degree of supersaturation. Whether or not silica dissolution around the injection well leads to the formation of cavities and consequent movement of well casings depends on the dissolution rate of

quartz (as influenced by temperature and pH) and the fluid injection rate. The probability of the occurrence of this type of problem can be minimized by maintaining the pH and the temperature of the injected fluids at their lowest practical level.

EXPERIMENTAL

STARTING MATERIALS

Sand

Oil sand from the McMurray formation was obtained from the GCOS mine site near Fort McMurray, Alberta, Canada. The bitumen was extracted with toluene by the Dean and Stark method and the bitumen-free sand was thoroughly mixed. Batch A consisted of a composite sample obtained from different barrels whereas Batch B was obtained from one barrel. These batches were divided into samples of the required weight using a sample splitter. The chemical composition of Batch A is given in Table 2. In a number of dissolution experiments the sand remaining from previous runs was used. Some experiments were carried out with pure quartz sand (Fisher Co., silica sand, fine granular). The quartz sand used for one dissolution experiment was treated with hydrofluoric acid and washed with NaOH solutions of decreasing strength and finally with deionized water to remove the disturbed surface layers (VAN LIER et al, 1960). Oil sand from Batch B was homogenized by kneading in a polyethylene bag and quartered into subsamples that were used for the dissolution experiments carried out in the presence of bitumen.

Solutions

Experiments were conducted in deionized water, 0.01 M borax (pH = 8.7 at room temperature) and in solutions that were brought to pH 6.5 and pH 7.5 by the addition of HCl to 0.01 M borax. The buffer capacity of these solutions is probably not great. However, it was

Table 2. Chemical Composition of Oil Sand Batch A (% by Weight)

SiO_2	97.01
Al_2O_3	1.05
Fe_2O_3(total)	0.14
TiO_2	0.15
P_2O_5	0.00
MgO	0.00
CaO	0.08
MnO	0.00
Na_2O	0.22
K_2O	0.34
Loss on ignition	0.63
H_2O	0.05
	99.67

Mineralogical Composition:

Mainly quartz. Very small amounts of kaolinite, illite and rutile (only show up in <45 μm fraction).

felt that the use of a different type of buffer solution could affect the dissolution process and make comparisons between sets of experiments of questionable value. One set of experiments was conducted in 0.01 M borax solutions that had been previously "saturated" with bitumen by heating for 24 hours at run temperature, after which the autoclave was cooled and the bitumen removed.

EXPERIMENTAL PROCEDURES

Sampling

The requisite amounts of sand and solution were placed in 300 ml stainless steel autoclaves (Parr Co., Moline, Ill. USA) that were equipped with sampling system 1, shown in Figure 1.

They were placed in a forced convection oven (Fisher, Isotemp) at the desired temperature. At regular intervals the autoclaves were placed in the heating mantle shown in Figure 1 and connected to the sampling system. The autoclave heating mantle was preheated to run temperature and the sampling tube was preheated to 20°C below run temperature. Both the sampling tube and the erlenmeyer flask were evacuated, after which valves C and D were closed and valves A and B opened. Any liquid remaining in the sampling tube was then removed by closing valve B and blowing nitrogen through C. After sampling, the autoclave was immediately returned to the oven and the sampling tube was repeatedly washed with deionized water while still hot. Sampling system 1 was later replaced by sampling system 2, a schematic drawing of which is presented in Figure 2. The autoclave was placed in the heating mantle and connected as in system 1, and the valve on the autoclave opened. Then valve B was carefully opened so that a slow steady flow of liquid was achieved. The initial 5 mls of sample were discarded. The samples taken with sampling system 2 were immediately diluted with cold deionized water (that had been

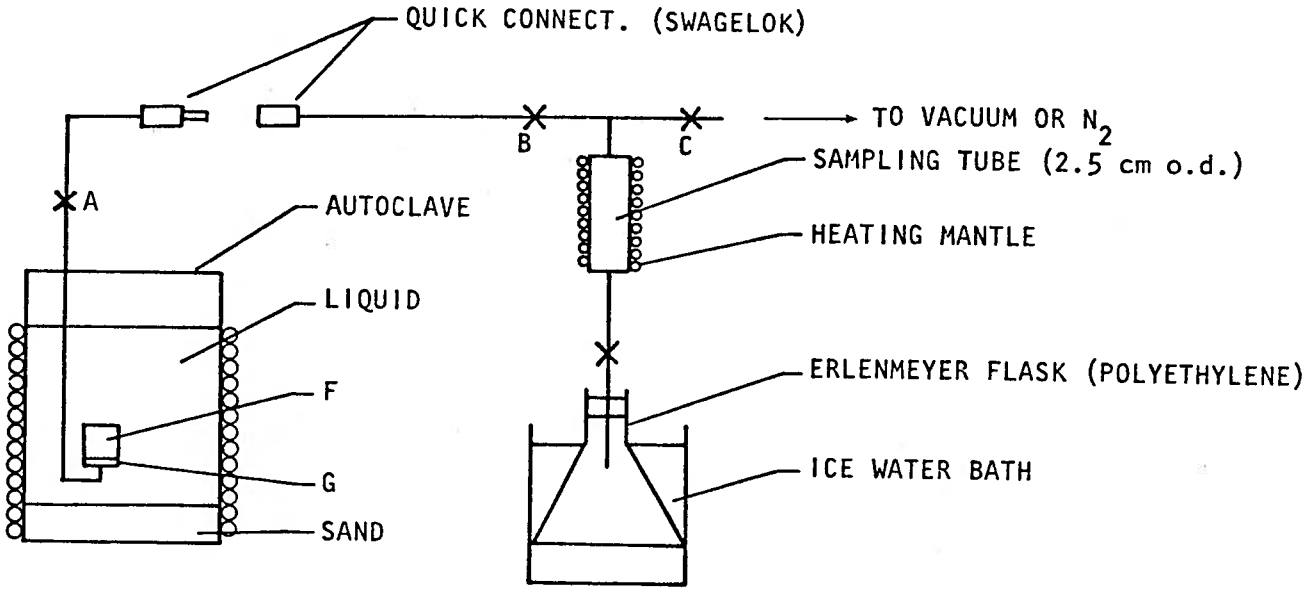

Figure 1. Autoclave and sampling system 1.

A, B, C, D: ball tip valves (Whitey NB series);

F: sintered stainless steel filter element, pore size 7 μm (Nupro);

G: filter element support

316 stainless steel tubing, 0.632 cm (¼") o.d. and 0.1645 cm (0.065") wall thickness.

Swagelok fittings were used throughout.

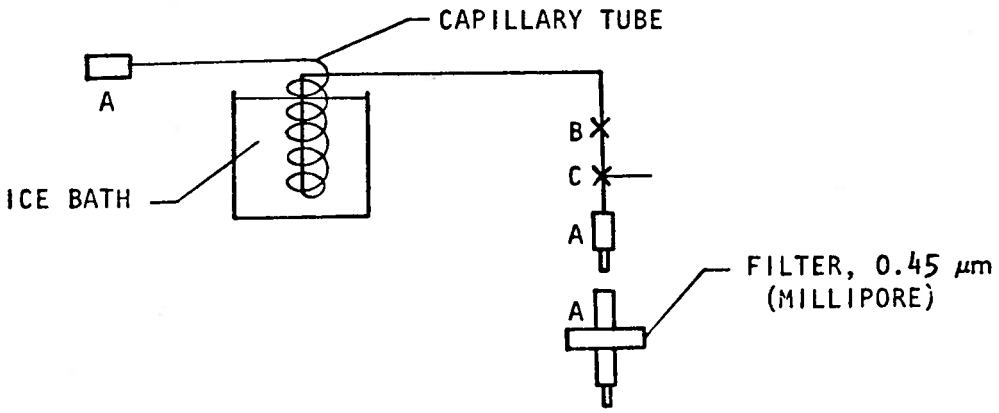

Figure 2. Sampling system 2.

A: Quick connect (Swagelok);

B: Regulating valve (Whitey SS-ORS2);

C: Cross Pattern Valve (Whitey SS-1VS4-X).

The stainless steel capillary tube has an o.d. of 0.1581 cm (1/16") and an i.d. of 0.109 cm. Valve C is used to release the pressure that builds up if the filter becomes clogged. The autoclave arrangement is the same as in system 1.

previously acidified with nitric acid) such that a final SiO_2 concentration of approximately 100 mg l^{-1} was obtained. The SiO_2 content of the solutions at room temperature was determined by atomic absorption spectrometry. The SiO_2 concentration did not vary with the time elapsed after sampling.

A 800 ml rocking bomb (Aminco 40-14375), equipped with a heating mantle was used for some experiments. The temperature of the rocking bomb was regulated by an automatic on-off controller. Samples were taken as described above.

Solid to Liquid Ratio

The effect of solid to liquid ratio on the dissolution rate was studied by reacting a fixed quantity of solution with varying amounts of sand and determining the SiO_2 concentration after a fixed, short time period.

Precipitation Rate

In one set of experiments, the solution was saturated with respect to quartz by heating with bitumen free oil sand or quartz sand at 280°C (static bombs) or 250°C (rocking bomb). The temperature was subsequently maintained constant at a lower level. The SiO_2 concentration was measured as a function of time. In a different set of experiments, solutions were saturated with amorphous silica (silicic acid, Fisher Scientific Co.,) at 130°C and at 100°C. These solutions were then maintained at 85°C and 25°C, respectively, in polyethylene elenmeyer flasks. Amorphous silica, quartz sand or bitumen free oil sand were added as nucleating agents. The solutions were stirred and the SiO_2 concentration was measured as a function of time.

Grain Surfaces

The surface area of the sand was determined by N_2 adsorption using BET isotherms with a Quantasorb Sorption system (Quantachrome Corp., Green Vale, N.Y., USA).

The surface of the sand grains was studied with a scanning electron microscope (Cambridge Instrument Co., Montreal, Que., Canada) that was equipped with an analytical spectrometer (Kevex Ray, Foster City, California).

Data Treatment

Equation (16) was fitted to the data that were obtained from the dissolution experiments.

$$-\ln (1 - C/C_{eq}) = Dt + B \tag{16}$$

where D and B are constants.

For the experiments conducted at pH $\leq$ 7.5, C_{eq} was calculated from equation (1). For the experiments in which 0.01 M borax was used, C_{eq} was taken as the average of the measured equilibrium concentrations. The curve-fitting procedure determines the values of D and B for which the function E^2 has a minimum (equation 17).

$$E^2 = \sum_{i=1}^{N} \frac{(Y_i - \overline{Y}_i)^2 W_i}{N - 2} \tag{17}$$

where:

$Y_i = -\ln (1-C_i/C_{eq})$, where C_i is the measured concentration for data point i

$\overline{Y}_i$ = calculated value of Y_i

N = number of data points

W_i = weight factor, calculated from C_i, the experimental error, using equations (18) and (19).

$$\Delta Y_i = \Delta C_i/(C_{eq} - C_i) \quad (18)$$

$$W_i = 1/(\Delta Y_i)^2 \quad (19)$$

The standard deviation in the measured equilibrium concentrations at pH < 7.5 was 19 mg l^{-1}, whereas for the experiments in 0.01 M borax it was 38 mg l^{-1}. ΔC_i for these cases was set at 20 mg l^{-1} and 40 mg l^{-1}, respectively. If the measured equilibrium concentration exceeds the calculated equilibrium concentration, the expression under the logarithm becomes negative. When this occurred, the measured concentration C_i was arbitrarily changed into $C_i = C_{eq} - 0.01$, which results in a very small weight factor for those particular data points. A fit was deemed satisfactory if $|Y_i - \overline{Y}_i| < \Delta Y_i$ for all i. Generally, this corresponded to $E^2 < 1$.

The activation energy for dissolution was obtained from the slope of an ln k_1S/V versus 1/T plot, where T is the absolute temperature. The slope was determined by the weighted least squares fitting procedure described above. An improved data treatment method is discussed in the appendix.

RESULTS AND DISCUSSION

DISSOLUTION EXPERIMENTS

Dissolution Rate

The values of D and B that were obtained from the dissolution experiments are given in Table 3, together with their standard deviations. This table also contains the calculated values of a number of derived parameters. Figure 3 shows a plot of ln k_1S/V

Table 3. Curve-fitting results. QTZ.S = quartz sand; CL.S = oil sand from which the bitumen has been extracted; OIL S. = oil sand; BIT.SAT.BOR. = bitumen-saturated borax; RB = rocking bomb; HF-TR = treated with hydrofluoric acid; SFPE = sand from previous experiment. Symbols preceeded by the letter D indicate the standard deviation of the parameter in the previous column. CO = C_{eq} [1=exp(-B)]. Units: CEQ:µg:Cm^{-3}; D:hr^{-1}; k_1S/V:µg cm^{-3}/hr^{-1}.

	EXPERIMENT	BATCH	CEQ	E SQ	1000D	1000DD	B	DB	k_1S/V	Dk_1S/V	LNk_1S/V	DLN	CO	DCO
1	QTZ S. DEION. H2O 20 G/L 250C. RB		415.4	1.00	6.24	0.72	0.355	0.050	2.59	0.30	0.95	0.12	124.1	14.6
2	QTZ S. DEION. H2O 13.3G/L 250C. HF-TR		422.2	0.09	5.04	0.57	-0.067	0.065	2.13	0.24	0.75	0.11	-29.1	29.3
3	CL. S. DEION. H2O 66.7G/L 150C.	A	129.1	0.12	3.22	1.29	0.169	0.161	0.42	0.17	-0.88	0.40	20.1	17.6
4	CL. S. DEION. H2O 66.7G/L 170C.	A	174.8	0.04	7.60	2.37	0.079	0.096	1.33	0.42	0.28	0.31	13.3	15.5
5	CL. S. DEION. H2O 66.7G/L 205C.	A	270.5	0.50	11.59	2.94	0.255	0.131	3.14	0.79	1.14	0.25	60.9	27.4
6	CL. S. DEION. H2O 66.7G/L 250C.	A	415.4	0.18	30.89	4.68	0.482	0.077	12.83	1.94	2.55	0.15	159.0	19.6
7	CL. S. DEION. H2O 20 G/L 250C. SFPE		415.4	0.06	73.37	9.54	-0.018	0.055	30.48	3.96	3.42	0.13	-7.4	23.1
8	CL. S. DEION. H2O 20 G/L 200C. RB	B	255.7	0.04	6.48	1.05	0.253	0.076	1.66	0.27	0.51	0.16	57.1	15.1
9	CL. S. DEION. H2O 20 G/L 200C. SFPE		255.7	0.20	10.34	1.67	0.029	0.075	2.64	0.43	0.97	0.16	7.4	18.7
10	CL. S. DEION. H2O 20 G/L 250C. RB	B	415.4	0.14	17.09	3.94	0.438	0.147	7.10	1.64	1.96	0.23	147.3	39.4
11	CL. S. DEION. H2O 20 G/L 250C. SFPE		415.4	0.23	21.25	2.91	0.248	0.070	8.83	1.21	2.18	0.14	91.3	22.6
12	CL. S. DEION. H2O 20 G/L 250C.	B	415.4	0.32	57.52	4.52	0.010	0.043	23.89	1.88	3.17	0.08	4.3	17.6
13	CL. S. DEION. H2O 20 G/L 255C. SFPE		432.6	0.32	39.59	5.61	0.142	0.047	17.12	2.43	2.84	0.14	57.4	17.7
14	CL. S. DEION. H2O 20 G/L 255C.	B	432.6	0.24	40.43	2.76	0.001	0.034	17.49	1.19	2.86	0.07	0.4	14.9
15	CL. S. PH 6.5 20 G/L 200C.	B	255.7	0.67	7.25	1.14	0.223	0.082	1.85	0.29	0.62	0.16	51.1	16.9
16	CL. S. PH 6.5 20 G/L 250C.	B	415.4	1.19	16.76	1.84	0.264	0.061	6.96	0.76	1.94	0.11	96.5	19.3
17	CL. S. PH 7.5 20 G/L 200C.	B	255.7	0.53	7.40	1.14	0.306	0.075	1.89	0.29	0.64	0.15	67.5	14.1
18	CL. S. PH 7.5 20 G/L 250C.	B	415.4	0.30	11.50	1.36	0.414	0.059	4.78	0.56	1.56	0.12	140.7	16.2
19	CL. S. 0.01M BORAX 20 G/L 200C.	B	467.0	1.99	6.88	0.63	0.267	0.035	3.21	0.29	1.17	0.09	109.5	12.7
20	CL. S. 0.01M BORAX 66.7G/L 250C.	A	764.7	0.60	32.36	4.38	0.261	0.059	24.75	3.35	3.21	0.14	175.8	35.0
21	CL. S. 0.01M BORAX 20 G/L 250C.	B	764.7	3.85	50.95	4.10	0.097	0.019	38.96	3.14	3.66	0.08	70.7	13.4
22	OIL S. DEION. H2O 20 G/L 200C.	B	255.7	0.41	4.58	0.60	0.186	0.062	1.17	0.15	0.16	0.13	43.3	13.2
23	OIL S. DEION. H2O 66.7G/L 250C.	B	415.4	0.83	9.58	1.85	0.485	0.063	3.98	0.77	1.38	0.19	159.6	16.1
24	OIL S. PH 6.5 20 G/L 200C.	B	255.7	0.31	6.25	0.89	0.322	0.074	1.60	0.23	0.47	0.14	70.4	13.8
25	OIL S. PH 6.5 20 G/L 250C.	B	415.4	0.87	8.56	1.27	0.355	0.061	3.55	0.53	1.27	0.15	124.0	17.7
26	OIL S. PH 7.5 20 G/L 200C.	B	255.7	0.24	4.30	0.65	0.304	0.078	1.10	0.17	0.09	0.15	67.1	14.7
27	OIL S. PH 7.5 20 G/L 250C.	B	415.4	1.03	11.32	1.08	0.261	0.041	4.70	0.45	1.55	0.10	95.4	13.0
28	OIL S. 0.01M BORAX 20 G/L 200C.	B	471.0	0.42	7.54	0.85	0.337	0.038	3.55	0.40	1.27	0.11	134.9	12.7
29	OIL S. 0.01M BORAX 20 G/L 250C.	B	674.6	0.55	29.11	7.85	0.307	0.070	19.64	5.30	2.98	0.27	178.6	34.9
30	OIL S. 0.01M BORAX 20 G/L 250C.	B	803.1	0.17	24.80	2.81	0.286	0.063	19.91	2.26	2.99	0.11	199.6	38.3
31	CL. S. BIT.SAT.BOR. 20 G/L 200C.	B	417.0	0.26	6.93	1.01	0.317	0.059	2.89	0.42	1.06	0.15	113.4	18.0
32	CL. S. BIT.SAT.BOR. 20 G/L 250C.	B	650.5	0.06	69.12	17.55	0.126	0.190	44.96	11.42	3.81	0.25	77.2	108.9

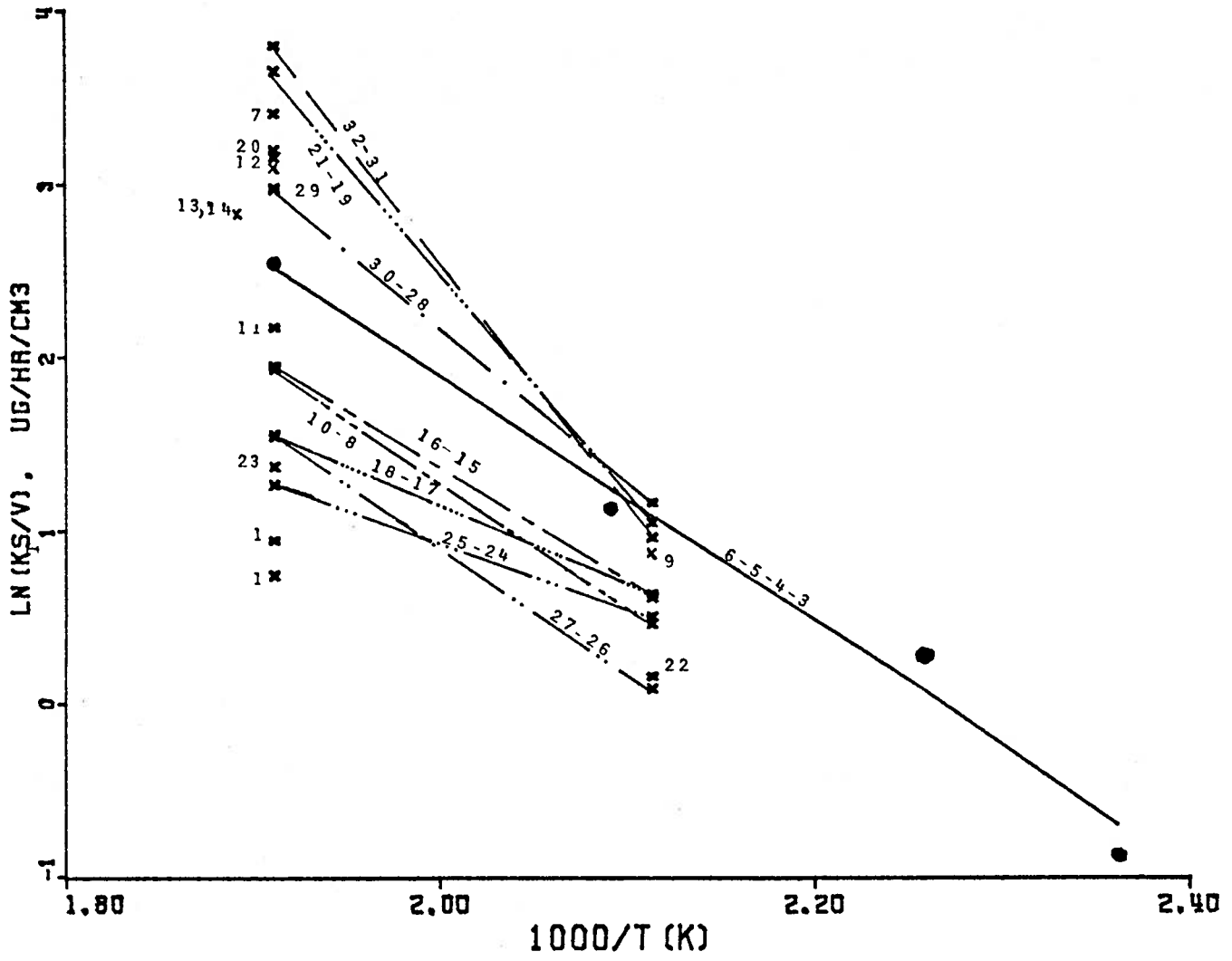

Figure 3. Arrhenius plot of dissolution rate constants. The numbers refer to the corresponding experiments in Table 2.

against 1/T. The activation energy for dissolution calculated from the slope of the line of best fit through the data points for experiments with bitumen-free oil sand and water (3 through 6) is 14.4 ± 1.4 kcal $mole^{-1}$. As will be discussed later in this report, the results of experiments in which the dissolution rate was measured as a function of solid to liquid ratio raised questions about the significance of the measured surface area in relation to the measured dissolution rate. It was also found that a significant fraction of the measured surface area is due to the presence of carbonaceous material in the oil sand. In view of these uncertainties about the correct value of S, attention was focused on k_1S/V rather than on k_1. In fitting a straight line to the ln k_1S/V versus 1/T data points and deriving the activation energy from its slope, the implicit assumption is made that S/V has the same value for all data points involved. For samples from the same batch and experiments with identical solid:liquid ratios, this assumption appears to be justified even though the small size of the sand samples may lead to a sampling error causing occasional deviations, as will be seen later in the report. Table 4 lists the activation energies calculated from the ln k_1S/V values for corresponding pairs of experiments. With two exceptions, the activation energies for dissolution are in the same range as that obtained from experiments 3 through 6 up to pH 7.5. The pH of the sampled solutions (measured at room temperature) varied in the ranges indicated below:

deionized water	pH 4.1 - 7.2
pH 6.5 "buffer" solution	pH 4.1 - 6.9
pH 7.5 "buffer" solution	pH 4.3 - 7.6

In general, the pH tended to increase with experiment duration, but fluctuations were observed. In deionized water, it took up to 400 hours for the pH to reach its final level and even then fluctuations were of the order of 1 pH-unit. With the pH 6.5 and pH 7.5 "buffer" solutions, the final pH range was reached within 80 hours and after that fluctuations were of the order of 0.4 pH units. In experiment 26 the pH went through a broad maximum at 7.4 from 80 hours to 200 hours and leveled off at 6.8 after 320 hours. The buffering capacity of the

TABLE 4

Calculated activation energies for dissolution for various pairs of experiments. Solid: liquid = 20 g l^{-1} in all cases.

Experimental Conditions	E_{act}	$\sigma_{E_{act}}$	Experiment Pair
Experimental Conditions	(kcal $mole^{-1}$)		
Cl. S. deion. H_2O rocking bomb	14.3	2.8	8 & 10
Cl. S. deion. H_2O sand from 8 & 10	12.0	2.1	9 & 11
Cl. S. pH 6.5	13.1	1.9	15 & 16
Cl. S. pH 7.5	9.1	1.9	17 & 18
Cl. S. 0.01 M borax	24.6	1.2	19 & 21
Oil S. pH 6.5	7.9	2.0	24 & 25
Oil S. pH 7.5	14.4	1.8	26 & 27
Oil S. 0.01 M borax	17.0	1.5	28 & 30
Cl. S. bit. sat. bor.	27.2	2.9	31 & 32

Cl. S. = clean sand

Oil S. = oil sand

bit. sat. bor. = 0.01 M borax previously saturated with bitumen at run temp.

solutions was apparently insufficient to compensate for the hydrogen ions released by the fluid-rock interactions that occurred. The initial lowering of the pH is probably caused by rapid cation exchange equilibration between clay minerals and solution. The released protons are subsequently consumed in clay mineral dissolution reactions. It was observed in two cases that the pH values measured in one bomb run were consistently lower (by 0.6 - 1.0 units) than those in a second bomb run at the same temperature using the same solution. This indicates that the sand samples used for the different runs were not identical and may have contained different amounts of clay minerals. The activation energies for experiment pairs 17 - 18 and 24 - 25 are probably erroneous, as they are closer to the range of values expected for diffusion controlled processes (RIMSTIDT, personal communication). The improved data treatment discussed in the appendix leads to an activation energy of 14.2 kcal $mole^{-1}$ for experiment pair 24-25. However, problems regarding the calculation of the standard deviation remain to be solved. Also, the value of 14 kcal $mole^{-1}$ is more in line with the results obtained by other authors (RIMSTIDT and BARNES, in press). At pH 8.7 the activation energy for dissolution of quartz is of the order of 25 kcal $mole^{-1}$, in reasonable agreement with the value of 21.7 kcal $mole^{-1}$ that was found in alkaline solutions by COURNOYER et al (1975). The higher value in alkaline solutions indicates a change in the mechanism of the dissolution reaction. The activation energy calculated from experiments 28 and 30 is somewhat low and may be erroneous.

New Mineral Formation

Scanning electron microscope studies showed that in all runs with 0.01 M borax, cubic crystals with trapezohedral truncations had grown on the surface of the quartz grains (plates 1-14). The size of these crystals increases with experiment duration and with temperature. They appear to start out as cubes and the trapezohedral truncations develop later. In a number of cases, spherical particles

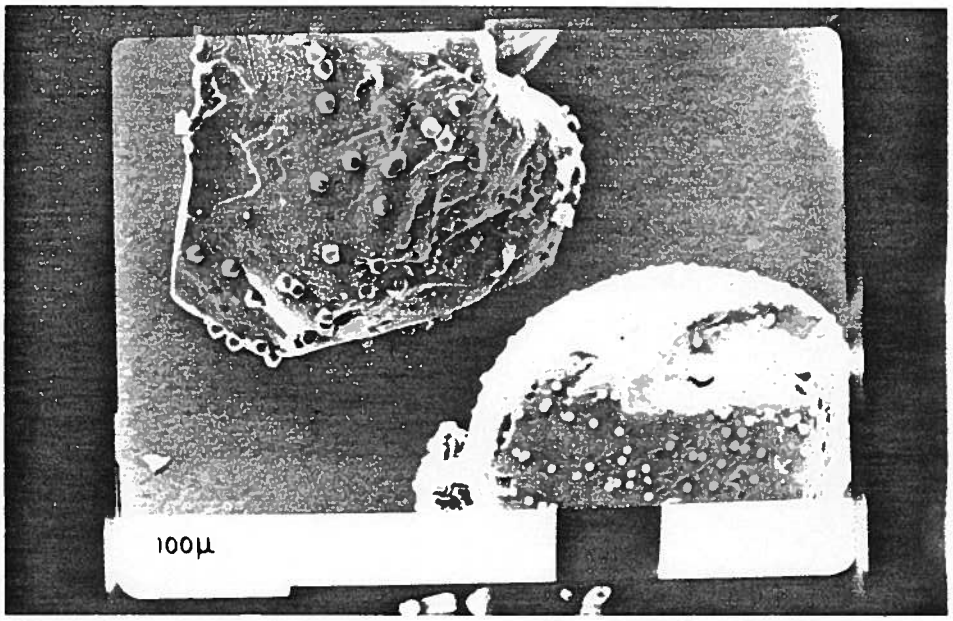

PLATE 1: Analcime crystals on top quartz grain, spherules on bottom quartz grain. Bitumen-free Athabasca sand reacted with 0.01 M borax at 252°C for 336 hours.

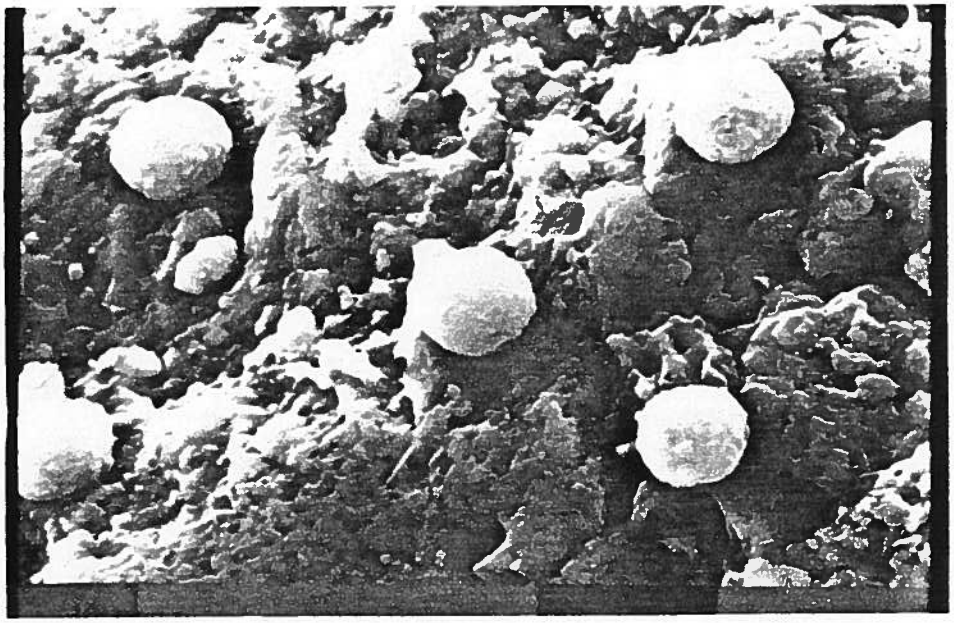

PLATE 2: Spherules on quartz. Note the irregular dissolution features on the quartz surface. Bitumen-free Athabasca sand, reacted with 0.01 M borax at 252°C for 257 hours.

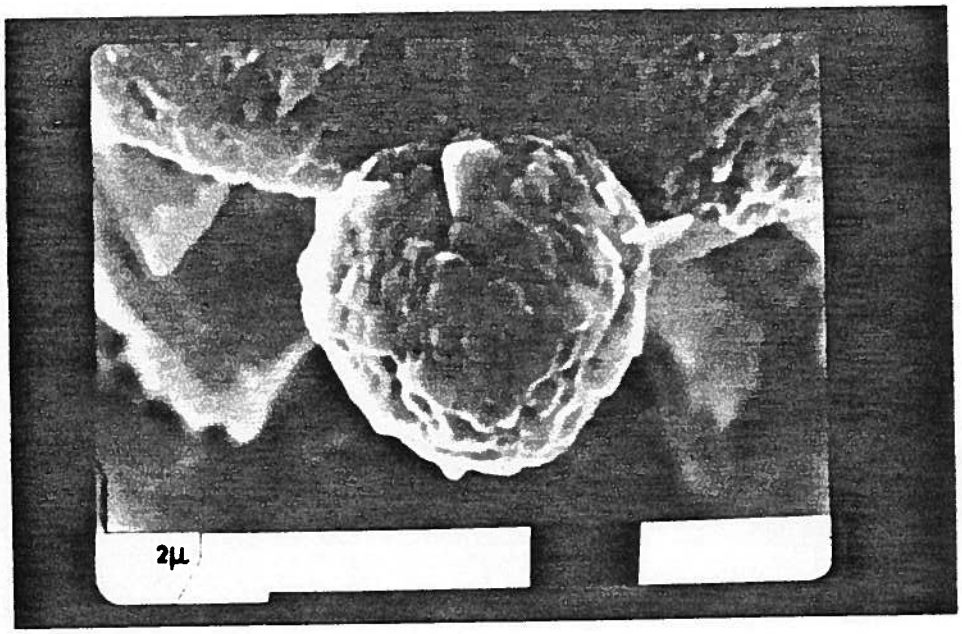

PLATE 3: Close-up of a spherule. Bitumen-free Athabasca sand, reacted with 0.01 M borax at 252°C for 336 hours.

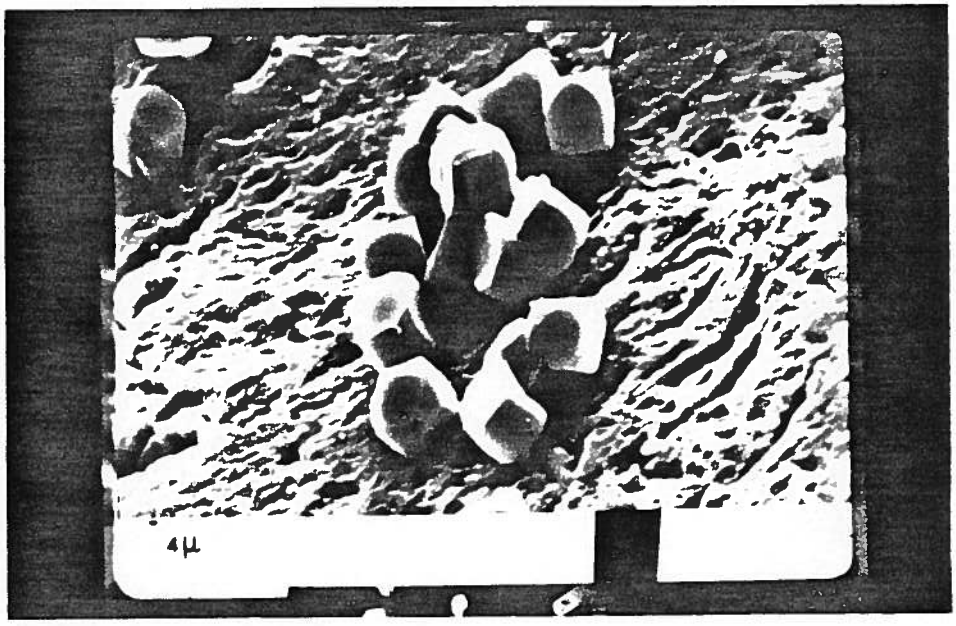

PLATE 4: Analcime crystals on quartz. Bitumen-free Athabasca sand, reacted with 0.01 M borax at 252°C for 30 hours.

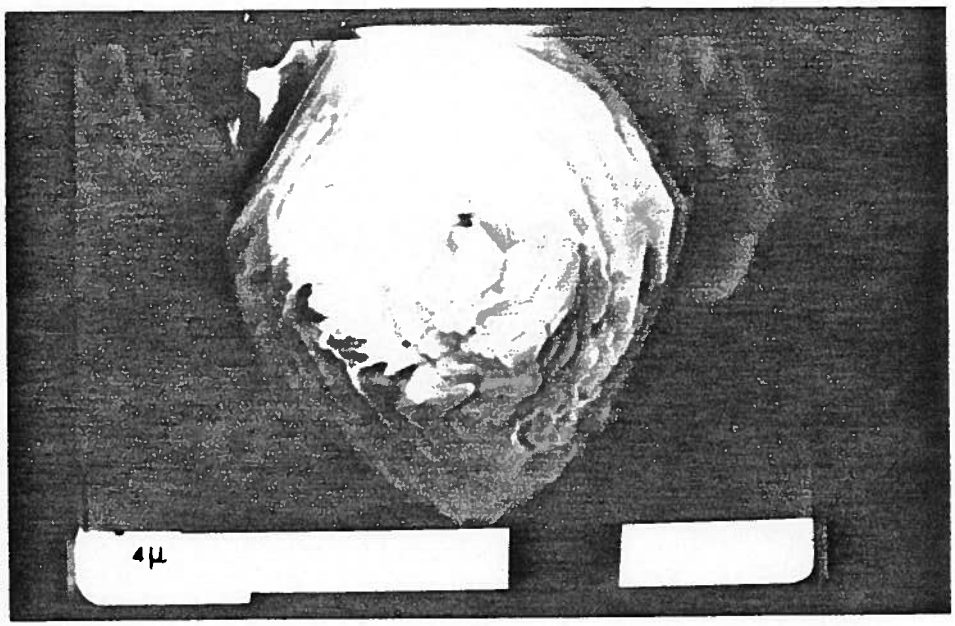

PLATE 5: "Imperfect" analcime crystal? Bitumen-free Athabasca sand, reacted with 0.01 M borax at 252°C for 336 hours.

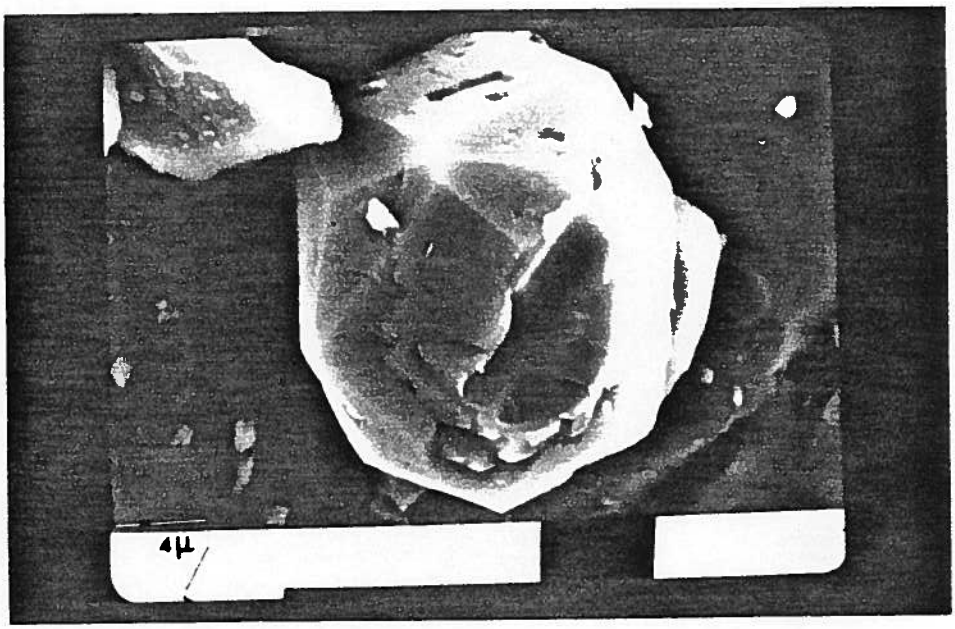

PLATE 6: Analcime crystal with growth imperfection. Bitumen-free Athabasca sand, reacted with 0.01 M borax at 252°C for 336 hours.

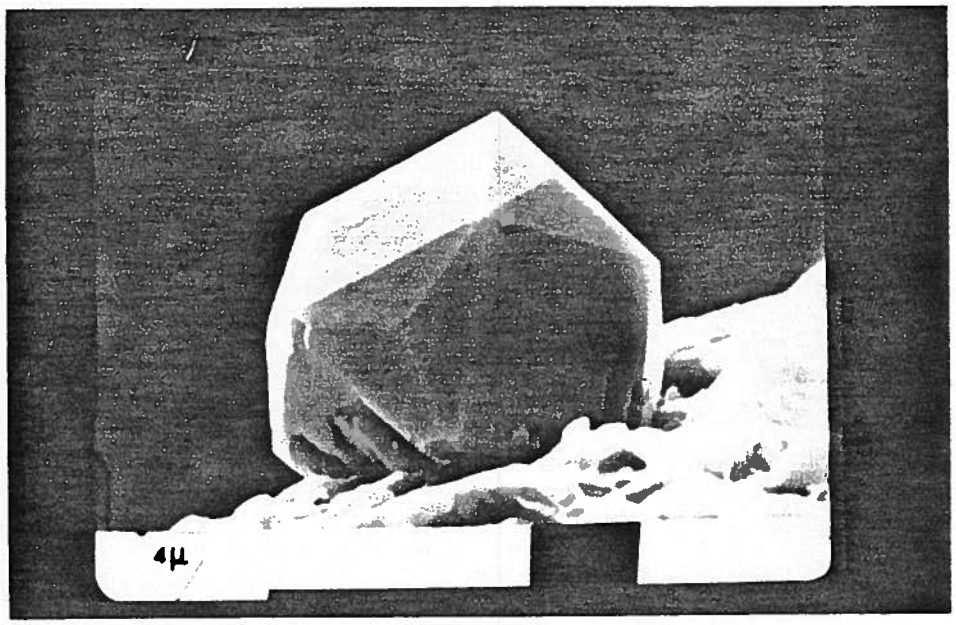

PLATE 7: Well-developed analcime crystal, Symmetry $\frac{4}{M}\ \bar{3}\ \frac{2}{M}$. Bitumen-free Athabasca sand, reacted with 0.01 M borax at 252°C for 336 hours. Note the increase in crystal dize with experiment duration, as compared to plate 4.

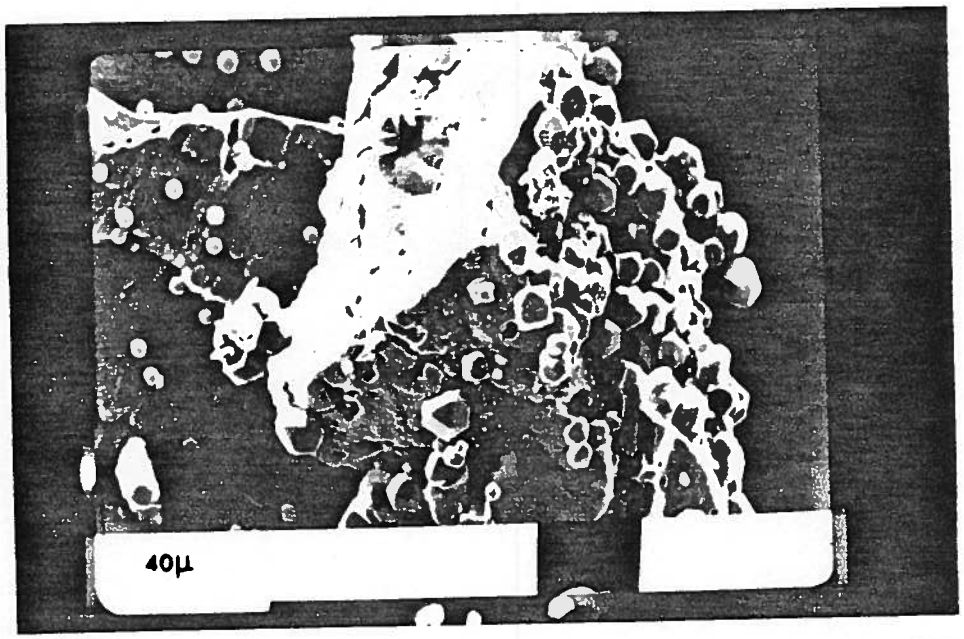

PLATE 8: Analcime crystals and spherules on quartz grains. Bitumen-free Athabasca sand, reacted with 0.01 M borax at 252°C for 336 hours. The overgrowth is quite dense.

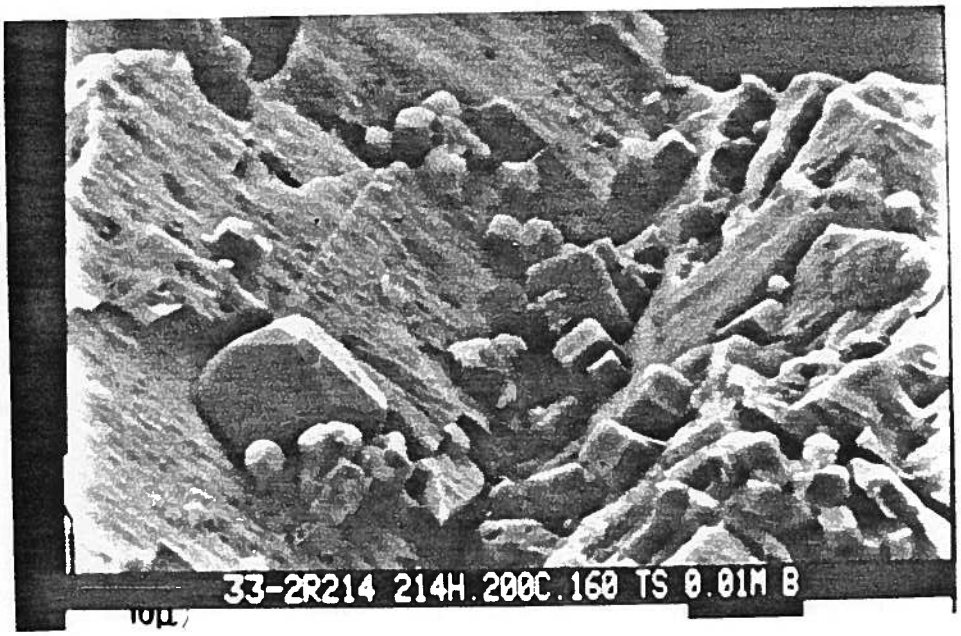

PLATE 9: Analcime crystals on quartz. Athabasca oil sand, reacted with 0.01 M borax at 200°C for 214 hours. There is a size distribution of crystals. Some crystals are intergrown. The smaller crystals seem to have less well developed trapezohedral truncations.

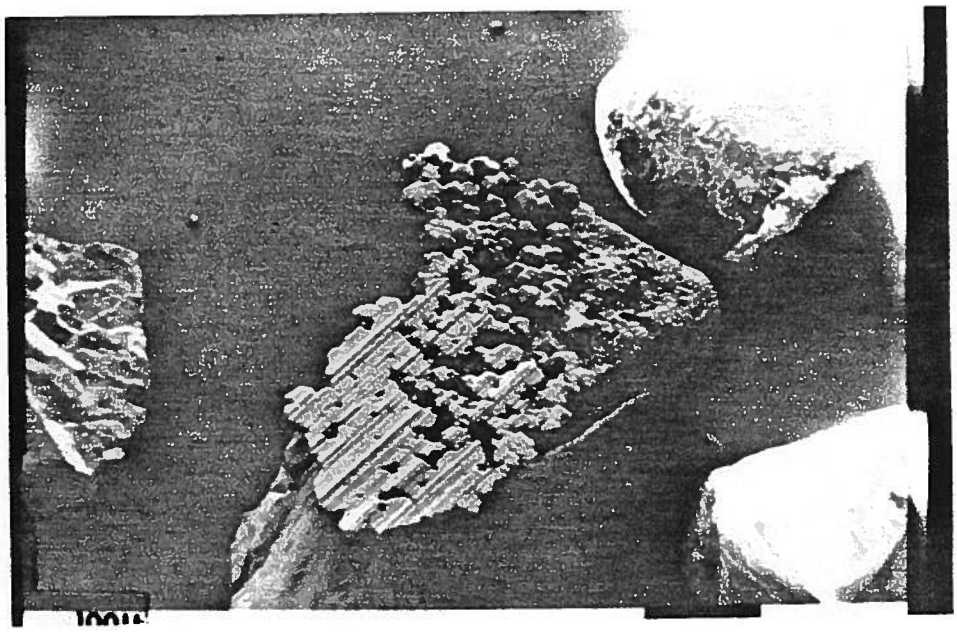

PLATE 10: Intergrown analcime crystals on quartz. Bitumen-free Athabasca sand, reacted with 0.01 M borax at 200°C for 408 hours.

PLATE 11: Extensive analcime growth closing off a pore. Bitumen-free Athabasca oil sand, reacted with 0.01 M borax at 200°C for 216 hours.

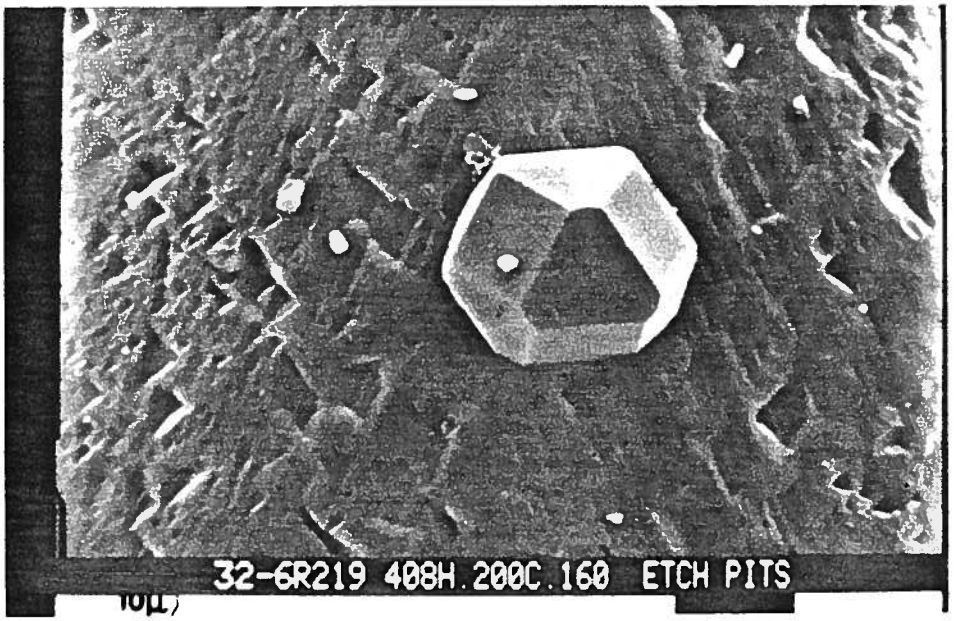

PLATE 12: Analcime crystal on quartz. Bitumen-free Athabasca sand, reacted with 0.01 M borax at 200°C for 408 hours. The v-shaped oriented depressions are caused by etching of the quartz surface (FRIEDMAN et al. 1976).

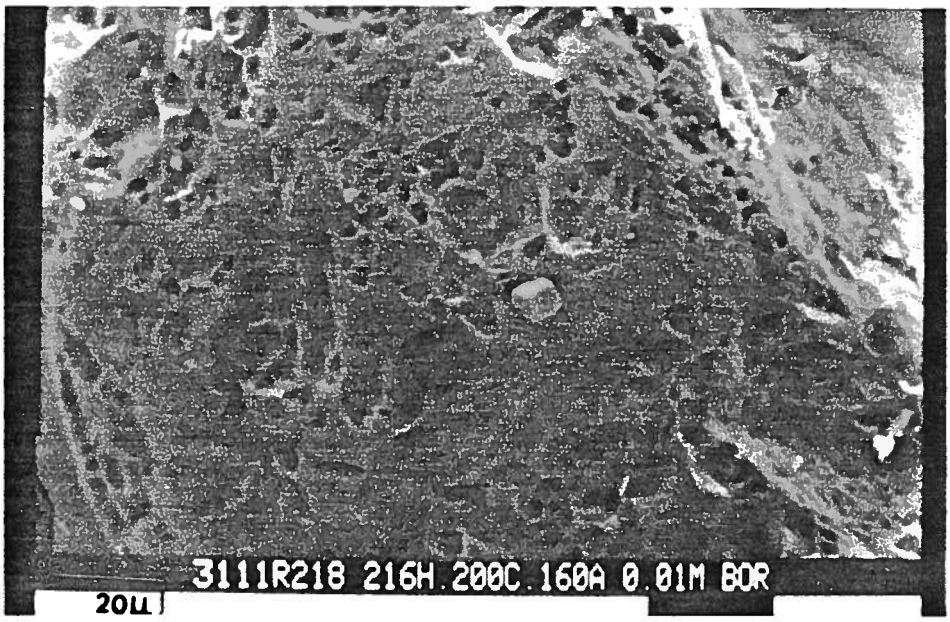

PLATE 13: Extensive etch pit formation on quartz surface. Bitumen-free Athabasca sand, reacted with 0.01 M borax at 200°C for 216 hours.

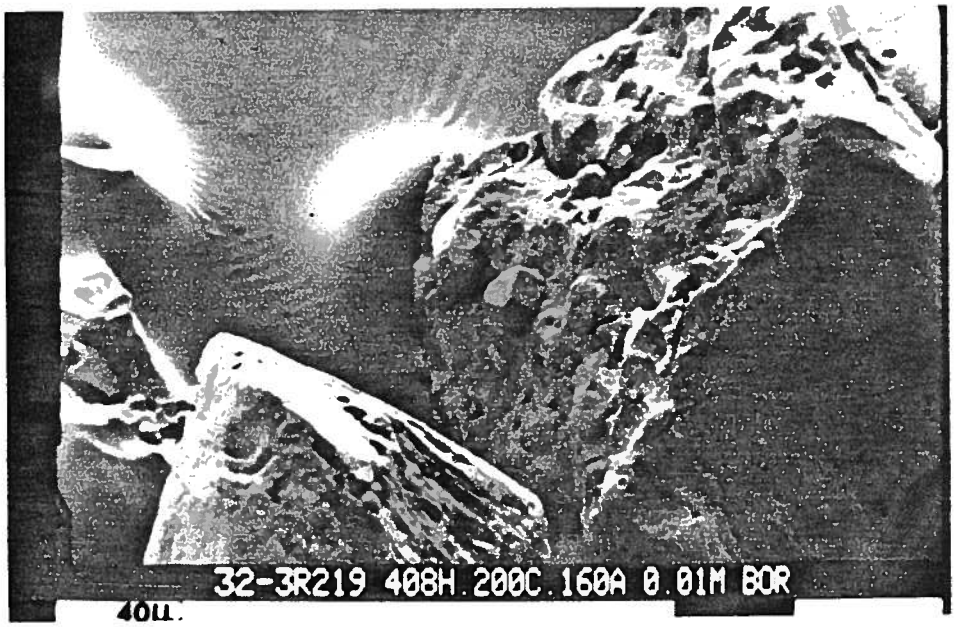

PLATE 14: Extensively etched quartz surface. Bitumen-free Athabasca sand, reacted with 0.01 M borax at 200°C for 408 hours.

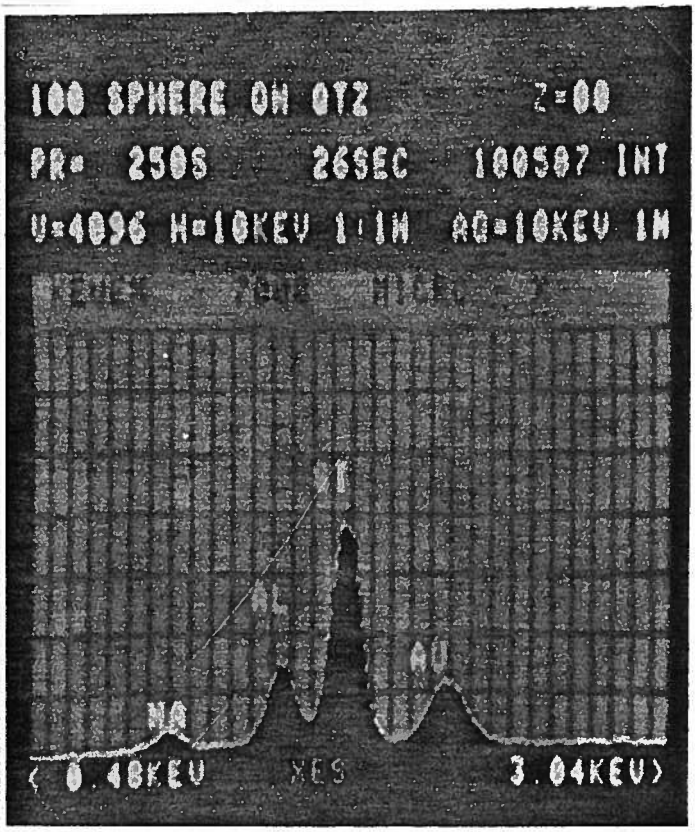

PLATE 15: X-ray spectrogram of a spherule. The specimen was coated with gold.

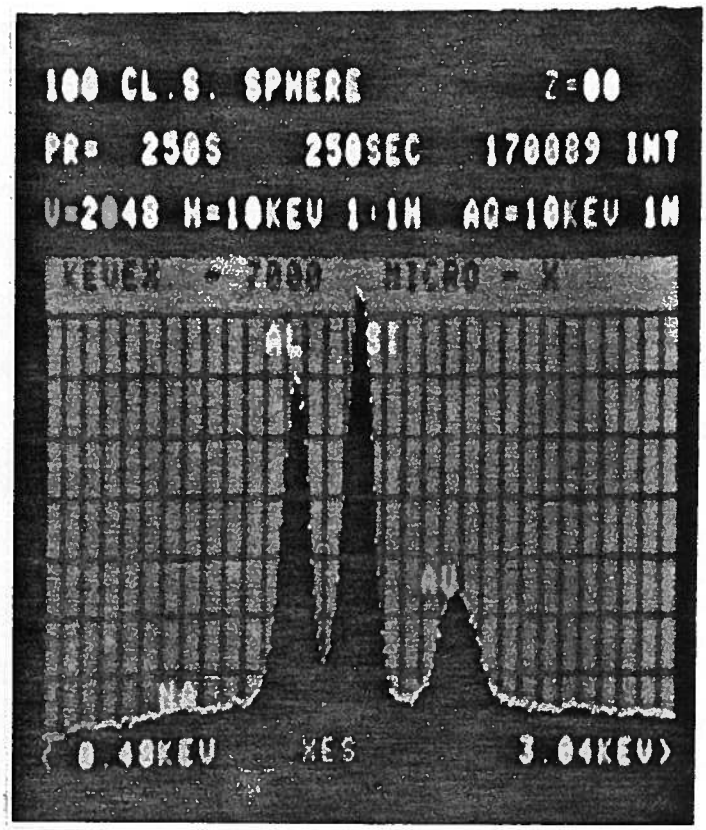

PLATE 16: X-ray spectrogram of a spherule. The specimen was coated with gold.

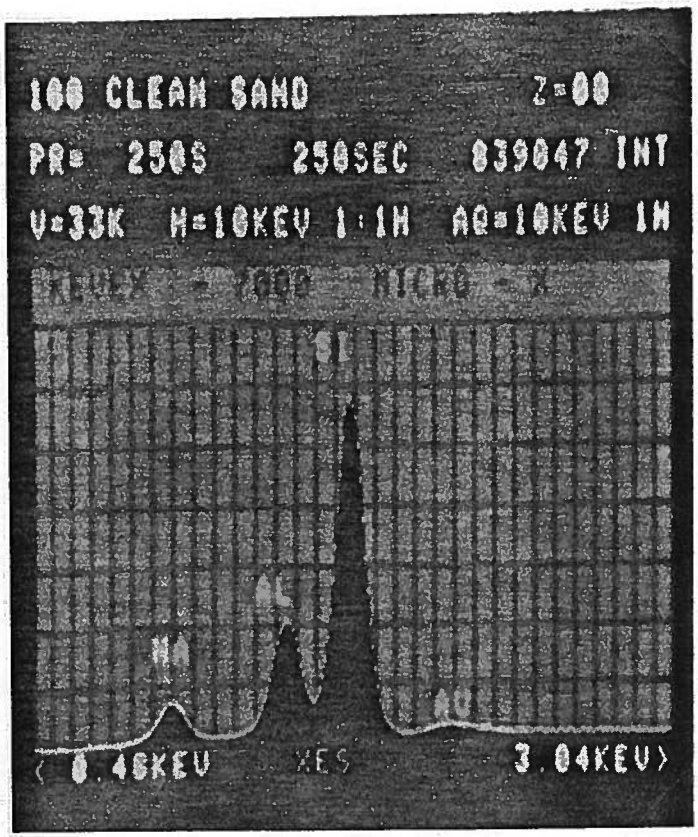

PLATE 17: X-ray spectrogram of an analcime crystal on quartz. The specimen was coated with gold.

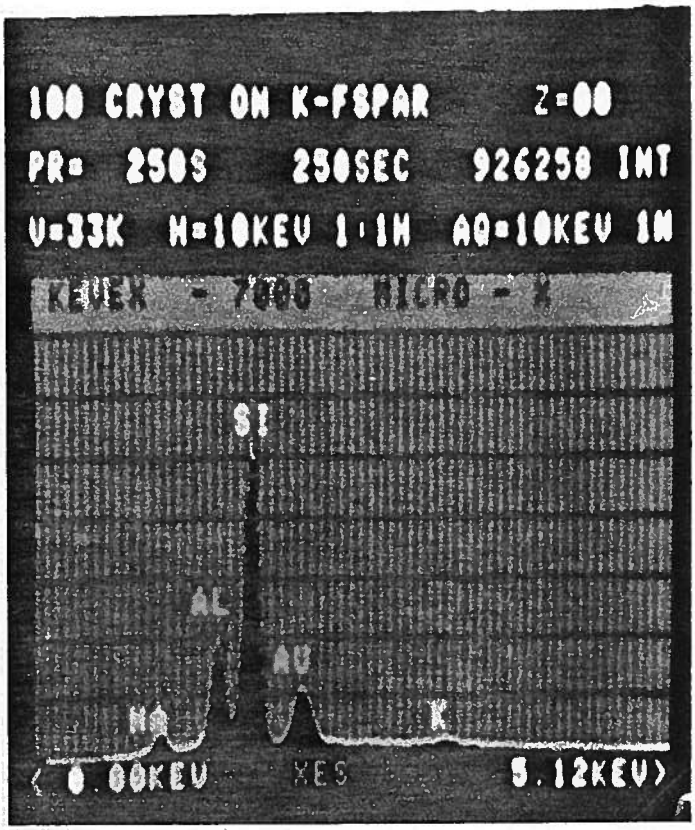

PLATE 18: X-ray spectrogram of an analcime crystal on K-feldspar. The specimen was coated with gold.

formed at the same time (plates 1 to 3). Spectrometric analyses indicated that Na, Al and Si are the main components of both spherules and crystals (plates 15 to 18). Both the composition and the crystal shape suggest that the crystals consist of analcime, $NaAlSi_2O_6 \cdot H_2O$. This conclusion was confirmed by powder X-ray diffractometry. Unfortunately, the amount of analcime in the sample was small in comparison to the amount of quartz which leads to a large uncertainty in the lattice parameter: $a = 13.6 \pm 0.15$ Å. For pure stoechiometric analcime $a = 13.71$ Å. COURNOYER et al (1975) synthesized analcime in the Na_2O-Al_2O_3-SiO_2-H_2O system by reacting quartz with alkaline aluminate solutions at 175 to 225°C at SiO_2/Al_2O_3 ratios between 6 to 36. These authors found that the rate-controlling step is the rate of supply of silica in solution. Obviously the consumption of silica by analcime formation interferes with the derivation of kinetic parameters from the experimental time-concentration data, but it is not known to what extent. Plates 8 - 11 show that extensive analcime growth can lead to the formation of agglomerates that may close off pores. The aluminum that is needed for the growth of the analcime crystals is probably provided by the dissolution of clay minerals and feldspars.

Effect of Bitumen

As Table 5 shows, bitumen lowers the dissolution rate of quartz in a number of cases. Surface adsorption of water-soluble components from the bitumen on the sand grains can be ruled out as a possible cause because the phenomenon was not observed when a "bitumen-saturated" borax solution was used. Extrapolation of density-temperature data for bitumen and observation of the flow of production fluids from the 150 cm physical simulator through a Jerguson cell indicate that at temperatures above 200°C the density of bitumen exceeds that of water. This means that, during the static bomb experiments, the bitumen remains at the bottom of the bomb and partially covers the sand grains and it is postulated that the surface area available for reaction is reduced by the physical adherence of bitumen to the sand.

TABLE 5

The effect of bitumen on ln kS/V

Δ(bit) = (ln kS/V) no bitumen - (ln kS/V) bitumen

Experimental Conditions			Δ(bit)	$\sigma_{\Delta(bit)}$	Experiment Pair
Deion H_2O	66.7 g l^{-1}	250°C	1.17	0.24	6 & 23
pH 6.5	20 g l^{-1}	200°C	0.15	0.21	15 & 24
pH 6.5	20 g l^{-1}	250°C	0.67	0.19	16 & 25
pH 7.5	20 g l^{-1}	200°C	0.55	0.21	17 & 26
pH 7.5	20 g l^{-1}	250°C	0.01	0.16	18 & 27
0.01 M borax	20 g l^{-1}	250°C	-0.10	0.14	19 & 28
0.01 M borax	20 g l^{-1}	250°C	0.67	0.14	21 & 30

The ln k_1S/V values for experiments 24 and 28 are higher than those of experiments with similar pH and temperature, whereas that of experiment 18 is lower. This leads to unreasonably low values of the activation energies calculated from pairs involving these experiments and to the absence of the bitumen effect in comparisons involving these experiments. The improved data treatment method discussed in the appendix leads to $\Delta(bit) = 0.38$ for experiment pair 19-28.

In each of these cases, the dissolution curve was obtained from three different bomb runs, the results of which agree with one another as is evident from the fact that $E^2 < 1$ in each case. Lack of reproducibility then does not seem to be the cause of the discrepancy.

Dissolution Stages

The positive B-values indicate that two dissolution processes are occurring one of which is virtually complete during the initial stages of the experiment. An estimate of the amount of SiO_2 dissolved during the initial rapid dissolution stage was obtained by calculating the SiO_2 concentration that would be present at $t = 0$, C_0, from equation (16). C_0 tends to increase with temperature and is higher for most experiments with 0.01 M borax (see Figure 4). In most cases C_0 is lower for repeated dissolution experiments on the same sand sample. Treatment of pure quartz sand with HF has a similar effect (see Table 2). These results agree with the literature reports that were cited on page 8. The large scatter in C_0-values indicates that the factors causing this phenomenon are not uniformly distributed throughout a bulk sand sample.

In experiments 7, 9 and 11 the slope of the line of best fit has increased with respect to the value found for the same sand sample in prior experiments 6, 8 and 10 which seems to indicate that the surface of the sand has been conditioned in some way by the quenching and drying that occurred between the two experiments. However,

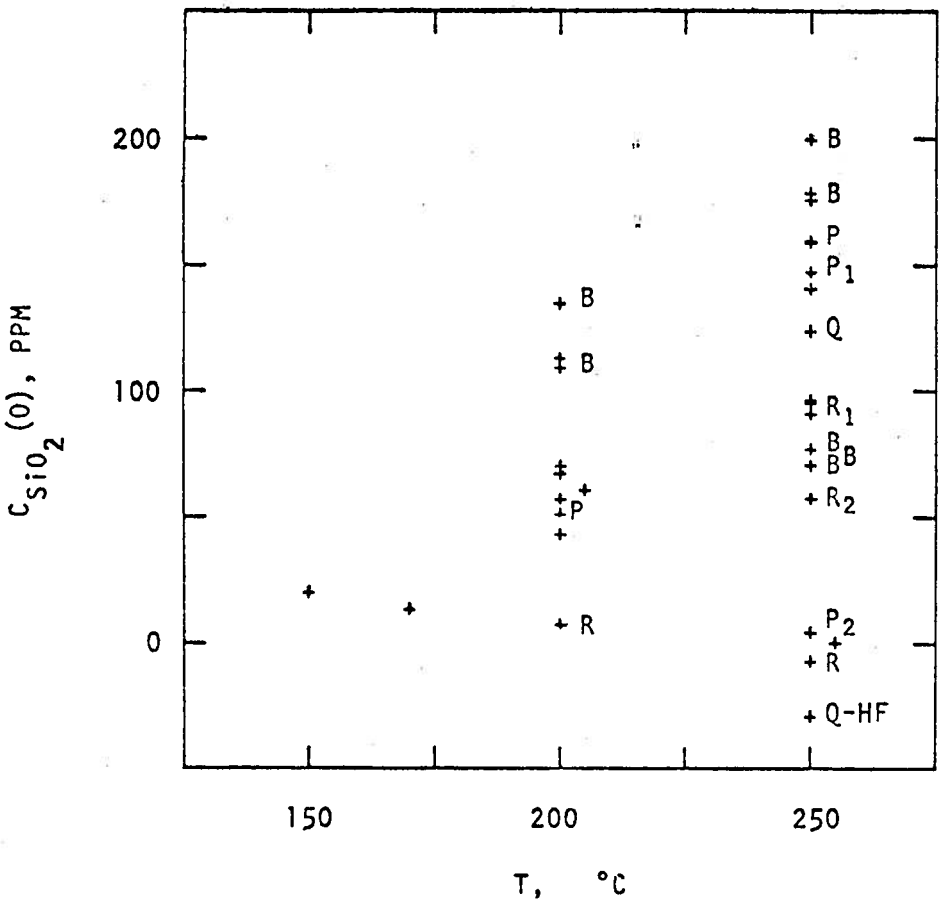

Figure 4. C_0 as a function of temperature.

B = experiments using 0.01 M borax;

Q = quartz sand;

Q-HF = HF-treated quartz sand;

R, R_1 and R_2 = experiments in which the sand from experiments P, P_1 and P_2 respectively was used.

experiments 12 and 13 show exactly the opposite results and k_1S/V for experiment 14 is almost identical to that for experiment 13. The values of k_1S/V for experiments 12, 13 and 14 are higher than those for other experiments at the same temperature and solid to liquid ratio and at a pH below 7.5. The sand for experiments 15 through 21 was taken from jar 160A, that for experiment 12 and 14 from jars 160B and 160E, respectively. The jars are subsamples of Batch B (see experimental section). It is possible that these subsamples are not identical and this may explain the higher k_1S/V values. It may be impossible to take "representative samples" that are small enough to be used for dissolution experiments.

Surface Area

The quartz sand that was treated with hydrofluoric acid had a surface area of 3000 cm^2g^{-1}. The surface area of a number of bitumen-free sand samples after the dissolution experiments ranged from 1000 to 7100 cm^2g^{-1}, the lowest values corresponding to the samples that had been reacted with 0.01 M borax. The carbonaceous material that was removed from the sand by gravity separation using a tetrabromoethane-acetone mixture had a surface area of 1750 cm^2g^{-1}. The bitumen-free oil sand contains less than one percent by weight of carbonaceous material and it was assumed initially that this does not contribute significantly to the total surface area of the sand.

However it was found that the surface area of a sand sample decreased from 6700 cm^2g^{-1} to 2200 cm^2g^{-1} by removing the carbonaceous material particles by hand. Apparently the tetrabromoethane treatment had decreased the surface area of the carbonaceous material. In order to be able to relate measured silica dissolution rates to the fraction of the sand surface area that takes part in the dissolution reaction it is necessary to remove all carbonaceous material. Gravity separation methods were found unsatisfactory because the fines remain suspended in the liquid for a very long time and it is difficult to avoid loss of fines. Sieving through a 32 mesh sieve removed most,

Table 6. Surface area of a number of one-gram sand samples taken from one jar. Most of the carbonaceous material was removed by sieving the sand through a 32 mesh sieve.

Sample Nr.	Surface Area ($cm^2\ g^{-1}$)
1	2500
2	2600
3	2600
4	2400
5	2400
6	2200
7	3200
8	3000

but not all of the carbonaceous material. The surface areas measured prior to the above observations cannot, therefore, be used to calculate k_1 from $k_1 S/V$. Table 6 lists the surface area of a number of one-gram bitumen free oil sand samples. The scatter in values is probably due to a sampling error caused by the small sample size.

Solid to Liquid Ratio

Diffusion may become the rate controlling step in the dissolution process when the dissolved SiO_2 has to diffuse through the intergranular pore system to reach the bulk of the liquid. The situation is schematically represented in Figure 5.

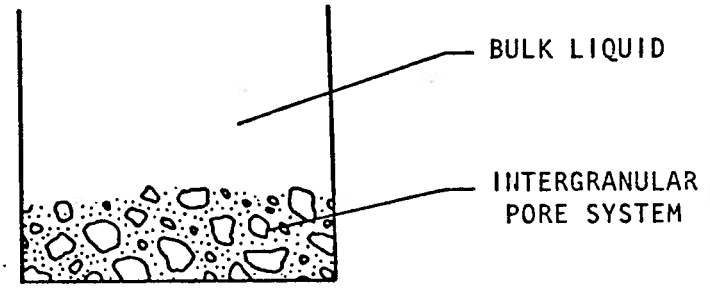

Figure 5. Schematic representation of the intergranular pore system in the sand.

The total diffusional flux perpendicular to the pore walls is much larger than that along the length of the pores because of the great difference in cross sectional area. The activation energy for diffusion-controlled processes is much lower than that for reaction controlled processes. This means that the rate of supply of SiO_2 into the intergranular fluid increases much faster with temperature than does the rate of diffusion out of the pores into the bulk fluid and, at a certain temperature, the latter may become smaller than the former in the part of the pore system that is farthest away from the bulk phase. The tortuosity of the pores further enhances the probability that this occurs. The effect of this phenomenon on the rate of SiO_2 concentration increase in the bulk liquid phase can be

expressed as a fractional decrease in the effective surface area. The importance of this phenomenon increases with the pore length (which in turn, increases with the solid to liquid ratio) and with the dissolution rate (which increases with temperature and pH). Figures 6 and 7 show the results of the experiments in which the SiO_2 concentration was measured after a fixed time period for different solid:liquid ratios. From equations (14) and (16):

$$D = \frac{k_1 \times S}{C_{eq} \times V} \tag{20}$$

Equation (20) can be transformed into equation (21):

$$D = \frac{k_1 \times r \times A'}{1000 \times C_{eq}} \tag{21}$$

k_1 = quartz dissolution rate constant ($\mu g\ SiO_2\ cm^{-2} hr^{-1}$)
r = solid to liquid ratio ($g\ l^{-1}$)
A' = specific surface area of the sand ($cm^2\ g^{-1}$)
C_{eq}= equilibrium SiO_2 concentration ($\mu g\ SiO_2\ cm^{-3}$)

Equation (16) becomes:

$$-\ln (1-C/C_{eq}) = \frac{k_1 \times A' \times t}{C_{eq} \times 1000} \times r + B' \tag{22}$$

$$= D' r + B'$$

Now t is a constant and C varies with the solid to liquid ratio. The value of $k_1 \times A'$ can be calculated from the slope of the least squares regression line through the data. C_0, the concentration calculated from (22) by setting $r = 0$, is closely related to C_0, the concentration calculated from (16) by setting $t = 0$. Using equations (20) and (21) $k_1 \times A'$ can be calculated from $k_1 S/V$ (see Table 3). The results of these calculations are listed in Table 7.

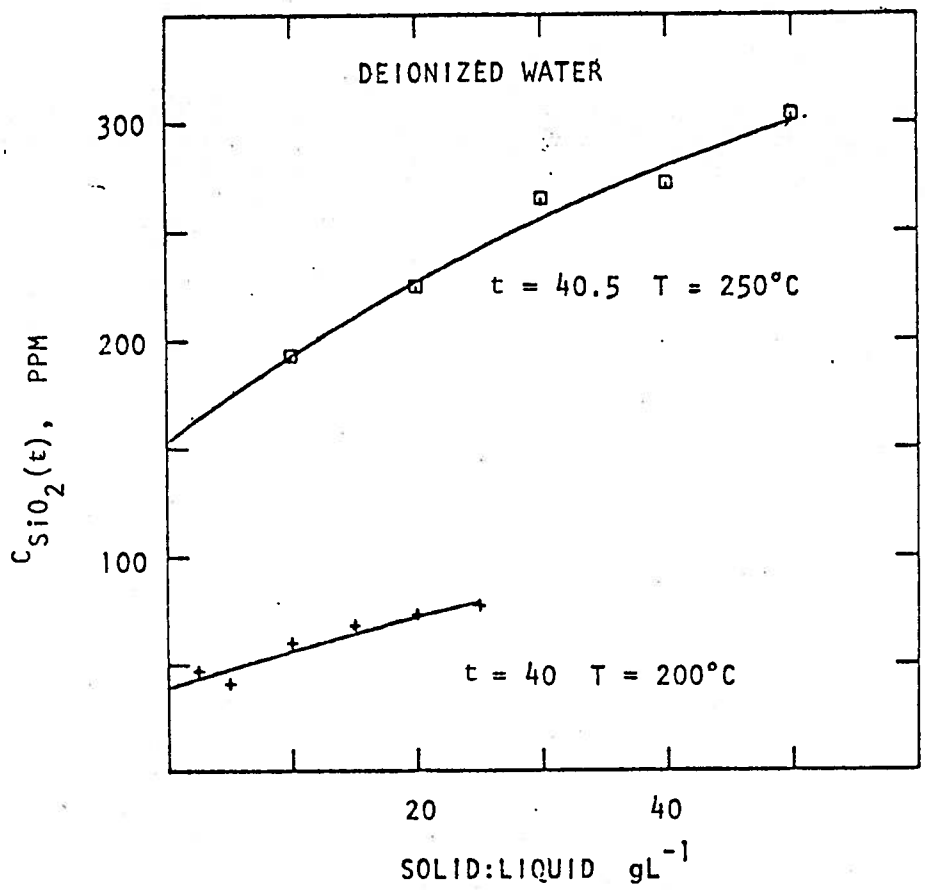

Figure 6. C_{SiO_2} measured after t hours as a function of solid:liquid ratio. The curves were obtained by fitting equation (22) to the maximum number of data points that could be included without obtaining a bad fit (see text). Experiments in deionized water.

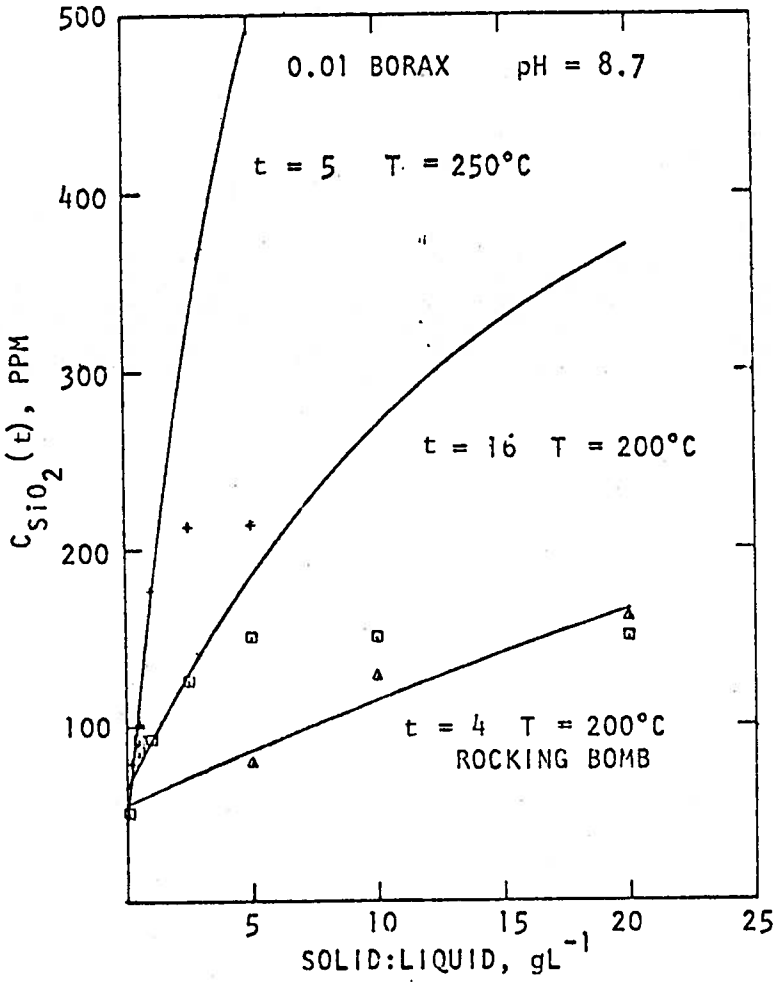

Figure 7. C_{SiO_2} measured after t hours as a function of solid:liquid ratio. Experiments in 0.01 M borax. Note the discrepancy between measured and calculated values for higher solid:liquid ratios for the static bomb.

TABLE 7

Parameters obtained by fitting $-\ln (1-C(r)/C_{eq}) = D'r + B'$ to the concentration vs solid to liquid ratio data obtained after t hours.

r = solid to liquid ratio (gl^{-1})

k_1 = quartz dissolution rate constant ($\mu g\ SiO_2\ cm^{-2}\ hr^{-1}$)

A^1 = specific surface area of the sand ($cm^2\ g^{-1}$)

E^2 = weighted mean square deviation

The standard error in C_{SiO_2} was set at 10 mg l^{-1} and 20 mg l^{-1} for the experiments in deionized water and in 0.01 M borax, respectively. S/L (max) indicates the maximum value of the solid to liquid ratio that was included in the least squares fit.

Experimental Conditions	t hrs	S/L(max) gl^{-1}	$1000D'$ lg^{-1}	$1000\sigma_{D'}$	$1000B'$	$1000\sigma_{B'}$	k_1xA' $\mu gSiO_2\ g^{-1}hr^{-1}$	$\sigma_{k_1xA'}$	C_0' μgcm^{-3}	$\sigma_{C_0'}$	E^2
Cl.S.Deion.	20	150	3.7	0.3	5.7	1.5	50	4	1.5	0.4	1.64
H_2O 205°C	20	66.7	5.8	0.6	24	17	78	8	6	5	0.31
	20	60.0	6.6	0.8	17	18	89	11	5	5	0.13
	20	32.0	7.5	1.4	10	20	101	19	3	5	0.08
Cl.S.Deion.	40	25.0	8.2	2.7	167	38	53	17	39	11	0.24
H_2O 200°C							(47)*	(12)*	(61)*	(27)*	
	40	20.0	110.8	4.5	136	59	69	29	33	13	0.15
Cl.S.Deion.	21	100.0	16.2	0.6	111	12	320	12	44	5	5.69
H_2O 250°C	21	75.0	17.0	0.7	104	13	337	14	41	5	5.09
	21	50.0	17.8	0.8	98	13	352	16	39	5	4.80
	21	20.0	25.8	1.6	58	15	510	32	23	6	1.51
	21	10.0	34.7	3.2	30.7	17.0	686	63	13	7	0.49
	21	5.0	41.7	8.0	19.2	20.9	825	158	8	9	0.08
Cl.S.Deion.	40.5	100.0	18.8	1.8	415	52	193	19	141	14	2.18
H_2O 250°C		75.0	17.8	2.0	435	54	183	21	147	15	1.75
		50.0	16.6	2.0	460	54	170	21	153	14	0.33
							(192)°	(29)°	(159)°	(20)°	
		40.0	15.9	2.6	471	61	163	27	156	15	0.30
		30.0	19.0	3.9	425	75	195	40	144	20	0.08
Cl.S. 0.01 M	16	20.0	26.9	6.7	192	23	779	196	81	9	7.04
Borax 200° C	16	2.5	7.4	29.8	149	34	2084	870	64	14	0.23
							(161)x	(15)x	(110)x	(13)x	
Cl.S. 0.01 M	5	5.0	45	9	145	20	6943	1331	104	13	4.20
Borax 250° C	5	2.5	96	19	108	24	14652	2936	78	16	1.3
	5	1.0	195	56	61	34	29823	8565	45	24	0.13
							(1948)+	(151)+	(71)+	(13)+	
Cl.S. 0.01 M											
Borax 200° C	4	20.0	15.6	5.5	127	67	1821	642	56	28	0.61

*, o, x and +: values from dissolution experiments during which time was varied at a constant solid to liquid ratio. (Experiments 5, 6, 19 and 21 in Table 3, respectively.)

The following observations can be made:

1. The calculated concentrations approach the measured concentrations more closely and the value of $k_1 \times A'$ is greater when only the lower range of solid to liquid ratios is considered, than when the whole range is taken into account. This is caused by the increase in pore length with increasing solid to liquid ratio and a consequent decrease in the effective surface area, as was discussed above.

2. In deionized water, at 205°C, the agreement between calculated and measured concentrations is good when only solid to liquid ratios < 66.7 g l^{-1} are included in the regression analysis. At 250°C, in deionized water and after 21 hours, the same holds true for solid to liquid ratios < 10 g l^{-1} whereas after 40.5 hours inclusion of solid to liquid ratios <50 g l^{-1} leads to reasonable agreement between calculated and experimental concentrations.

3. The $k_1 \times A'$ values obtrained from experiments with a 40-hour duration are smaller than those obtained from the experiments of shorter duration. The latter fall in the transition range between the initial rapid dissolution and later slower dissolution stages and consequently k_1 for these experiments is greater. The C_0-values increase with experiment duration because B (see equation 16) for the initial stages of dissolution is smaller than B for the entire dissolution process.

4. The $k_1 \times A'$ values obtained from the experiments in deionized water in which the solid to liquid ratio was varied (B and D, Table 7, t = 40 hours) compare favourably with those obtained from the experiments in which time was varied at a solid to liquid ratio of 66.7 g l^{-1} (bracketed values marked * and ° in Table 7). This indicates that, under these conditions, the effective surface area does not differ significantly from the total surface area.

5. The conclusion drawn under (4) does not apply to the experiments in 0.01 M borax. For these, satisfactory agreement between calculated and measured SiO_2 concentrations is obtained if only the solid to liquid ratios $\leqslant 2.5$ g l^{-1} at 200°C and $\leqslant 1.0$ g l^{-1} at 250°C are included in the regression analysis. At higher solid to liquid ratios, the effective surface area is much smaller than the total surface area. Assuming that the correct value of k_1 x A' (total) is obtained from the experiments in which the solid to liquid ratio was varied in the range specified above at constant reaction time, and designating the value of k_1 x A' obtained from the dissolution experiments in which time was varied at a constant solid to liquid ratio as k_1 x A' (effective) then:

- at 200°C and 20 g l^{-1}

$$\frac{A'(\text{effective})}{A'(\text{total})} = \frac{161 \pm 15}{2084 \pm 970} = 0.007 \pm 0.039$$

(see E, Table 7)

- at 250°C and 20 g l^{-1}

$$\frac{A'(\text{effective})}{A'(\text{total})} = \frac{1948 \pm 157}{1982 \pm 8565} = 0.065 \pm 0.024$$

(see F, Table 7)

In this case because of the high silica dissolution rate, the pore length at which the diffusional flux out of the pore becomes smaller than the rate of supply of silica into the pore by dissolution is much shorter than that for the experiments in deionized water.

6. The results obtained from the rocking bomb (see G, Table 7) support the explanation given under (5): In this experiment,

dissolved SiO_2 does not have to diffuse through the pore system to reach the bulk of the liquid and the calculated SiO_2 concentrations agree within the experimental error with the measured concentrations, at least up to a solid to liquid ratio of 20 g l^{-1}, and possibly higher. Also, $k_1 \times A'$ derived from this experiment is within experimental error equal to $k_1 \times A'$ derived from the corresponding experiments in static bombs over a much lower range of solid to liquid ratios (E, Table 7).

SUMMARY OF DISSOLUTION RESULTS

1. The dissolution of quartz is reaction-controlled. In static systems, diffusion out of the pore space into the bulk of the liquid may become the rate determining step for the fraction of the sand that is farthest away from the bulk liquid phase. Pore length, diameter, tortuosity and surface dissolution rate are the parameters that determine whether or not this situation will arise. In the present study, this phenomenon was found to be important at high pH when the solid:liquid ratio exceeds 1.0 g l^{-1} (at 250°C) or 2.5 g l^{-1} (at 200°C).

2. The dissolution process consists of an initial rapid stage, corresponding to the dissolution of a disturbed surface layer or of very fine particles adhering to the coarse grains and a later, slower stage during which the undisturbed quartz matrix dissolves. The amount of SiO_2 dissolved during the initial stage varies with temperature and pH and depends on sample history.

3. The activation energy for the dissolution of the undisturbed mineral matrix is 14.4 ± 1.4 kcal $mole^{-1}$ at pH < 7.5. At pH 8.7, the activation energy lies in the range 25 - 27 kcal $mole^{-1}$.

4. Both dissolution rate and equilibrium concentrations are much higher at pH 8.7 than at pH $\leq$ 7.5.

5. The SiO_2 dissolution rate is smaller in the presence of bitumen than in its absence and this is attributed to a reduction in the amount of SiO_2 surface area that is exposed to the solutions.

6. Carbonaceous material contriutes significantly to the total surface area of the sand.

7. At high pH, analcime crystals form on the surface of the quartz grains.

PRECIPITATION EXPERIMENTS

Amorphous Silica

Figure 8 shows the results for the precipitation of amorphous silica. The following conclusions can be drawn:

- There is an induction period during which nucleation takes place.

- The nucleation step is eliminated by seeding with amorphous silica.

- Quartz does not provide nucleation sites.

- The precipitation rate is decreased by the addition of bitumen-free oil sand. According to ALEXANDER (1954) the polymerization of silica is catalyzed by fluoride, even at concentrations as low as 1 mg l^{-1}. The deionized water that was used for the experiments contained approximatey this amount of fluoride and the aluminum ions liberated from the clay minerals in the oil sand form complex ions with the fluoride, thereby decreasing the catalytic effect of the latter.

- Nucleation is facilitated at higher temperatures.

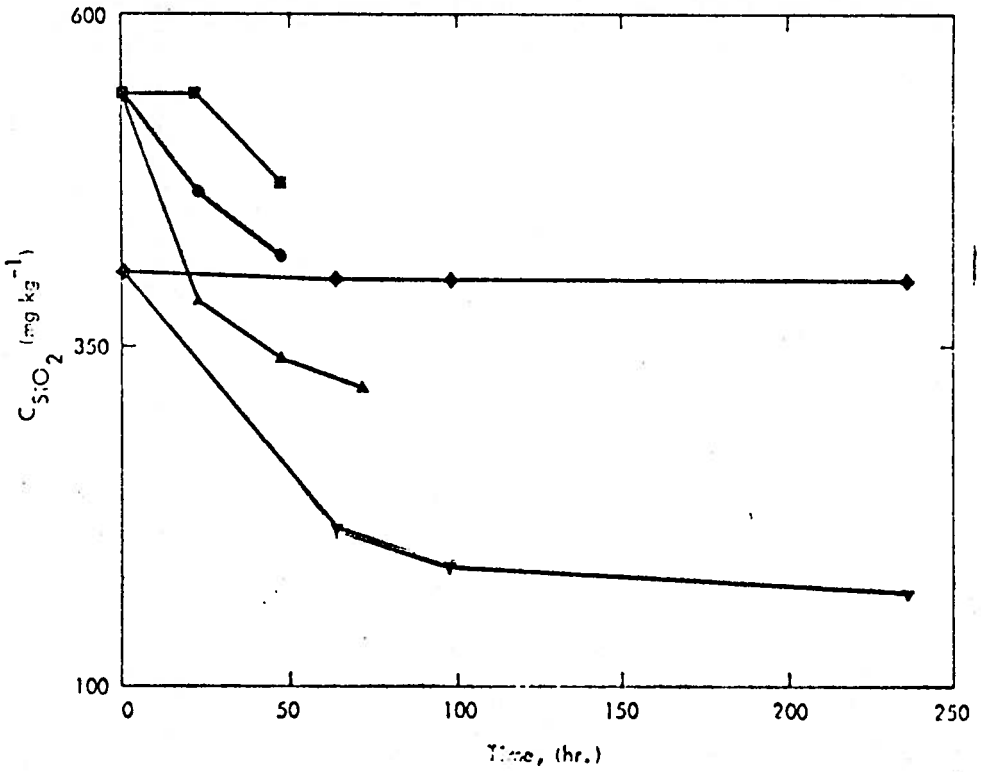

Figure 8. Precipitation of amorphous silica.

■ 85°C without seed.

◢ 85°C with amorphous SiO_2 seed.

● 85°C with amorphous SiO_2 seed and bitumen-free oil sand

◆ 23°C with quartz sand.

▼ 23°C with amorphous SiO_2 seed.

- The reaction times to equilibrium are short when compared with residence times of fluids in the formation during in situ recovery in the field. Amorphous silica precipitation will most likely occur in the vicinity of the production wells as this is the only region where the temperature of the fluids becomes low enough to cause supersaturation with respect to amorphous silica.

Quartz

Figure 9 shows the results that were obtained with the rocking bomb. Bitumen-free oil sand was reacted with deionized water at 250°C until an equilibrium concentration of 438 mg l^{-1} SiO_2 was reached. Then the temperature was lowered to 200°C and kept at that level for 520 hours. During this period, no precipitation took place. When the temperature was subsequently lowered to 150°C, precipitation started almost immediately and after 141 hours at 150°C the SiO_2 concentration had dropped to 130 mg l^{-1}, the equilibrium concentration of quartz at that temperature. Surprisingly, the concentration kept going down until after 360 hours a value of 32 mg l^{-1} was reached. Upon reheating to 250°C the concentration rose quickly and equilibrium was attained within 150 hours. In a second rocking bomb experiment, the solution was saturated at 200°C (248 mg l^{-1}) and the temperature was then lowered to 150°C. In this case, precipitation only started after more than 70 hours at 150°C and it took more than 300 hours to reach the equilibrium concentration of 130 mg l^{-1}. Again the silica concentration continued to decrease past its equilibrium value and reached 32 mg l^{-1} after 800 hours at 150°C, at which time the experiment was terminated. A similar experiment was carried out with pure quartz sand that was equilibrated with deionized water at 250°C after which the temperature was lowered to 150°C. Precipitation only started after more than 338 hours at 150°C. After 509 hours the concentration had reached 108 mg l^{-1}, again less than the equilibrium value. Unfortunately the experiment had to be interrupted at this point for logistic reasons. In all these experiments the pH varied between 5.7 and 7.4, increasing with increasing time.

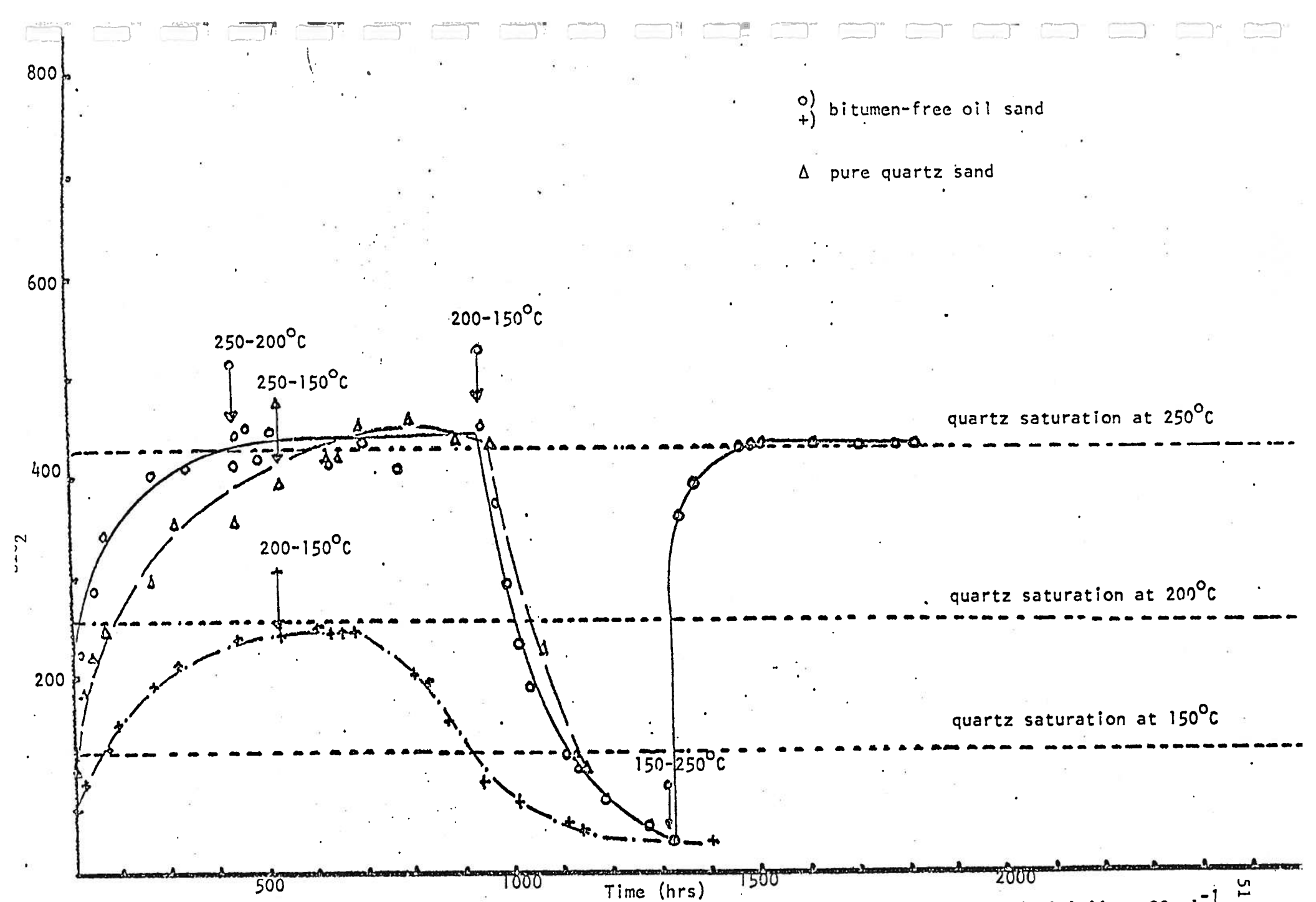

Figure 9: Dissolution and precipitation of SiO_2 from bitumen-free sand and pure quartz sand. Sol:liq = 20 gl^{-1}. The arrows indicate the time at which the indicated temperature changes were made. The experiments were carried out in the rocking bomb with deionized water.

It can be concluded that, at the conditions of pH and temperature employed:

- the precipitation rate increases with the degree of supersaturation

- The induction period decreases with increasing supersaturation.

An explanation for the fact that the SiO_2 concentration decreases to a value below the quartz equilibrium value has yet to be put forth. A similar phenomenon was observed by McCURDY, University of Lethbridge who carried out experiments with pure quartz sand (personal communication).

The results obtained with the static bombs are shown in Figure 10. Precipitation only started after 600 hours at all temperatures and after 900 hours had decreased to around 460 mg l^{-1}. Temperature did not seem to affect the results. Comparing these observations to the results obtained with the rocking bomb it appears that the rocking action enhances the precipitation rate. This means either that diffusion is the rate determining step or that abrasion of the sand grains in the rocking bomb provides better nucleation sites. Both sets of results disagree with those of RIMSTIDT and BARNES (personal communication) who studied the precipitation of quartz from solution during flow through a sand bed and found that equation (13) describes the rate of concentration change. Apparently the experimental set-up strongly influences the results.

As was mentioned before, the polymerization rate constant of silica has a maximum at pH 7.5 - 8. The polymerization reaction is second order at lower pH and third order at higher pH GOTO (1956); KITAHARA (1960). Consequently, the precipitation rate is expected to increase with pH. An indication of this effect was found in the results of experiments 20 and 21 (Table 3). The equilibrium concentration attained in the former was 535 mg l^{-1}, whereas in the latter it was 765 mg l^{-1}. Sampling system 1 was used for experiment 20 and sampling

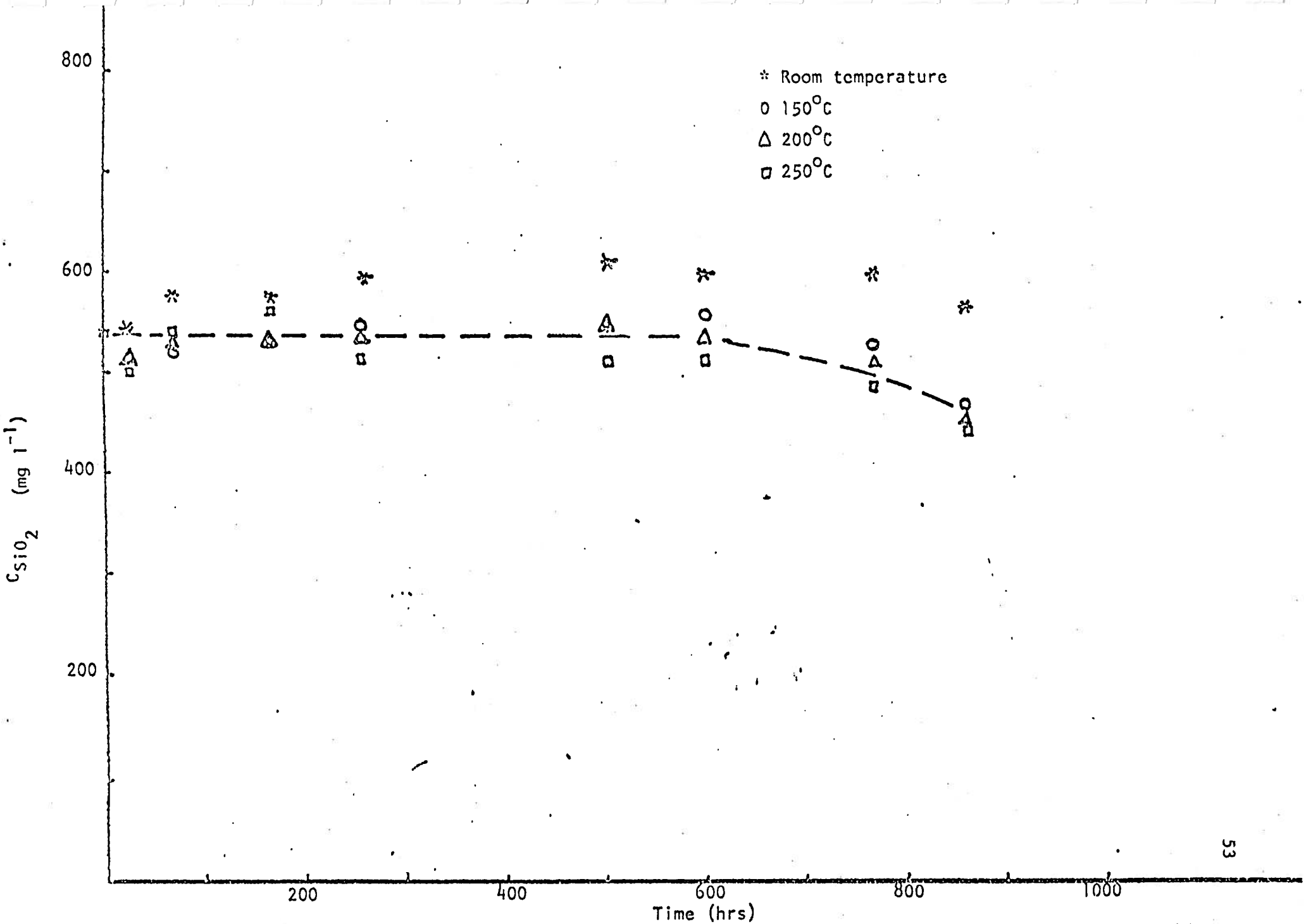

Figure 10: Precipitation of SiO_2 at different temperatures. Static bombs, deionized water. Solid:liquid 20g l^{-1}. Bitumen-free oil sand. Charges were equilibrated at 280°C.

system 2 for experiment 21. Quenching is much faster in sampling system 2 than in sampling system 1, where the sample is held for 15 - 30 seconds at 20°C below run temperature before being quenched and apparently this was long enough for precipitation to take place. It is possible that the larger scatter in equilibrium concentrations at high pH (standard deviation 38 mg l^{-1} as opposed to 19 mg l^{-1} for lower pH) can be explained in the same way: the flow rate during sampling and consequently the quench rate vary between experiments.

APPLICATION OF THE RESULTS

DISSOLUTION OF SiO_2 IN THE ARC 150 CM PHYSICAL SIMULATOR

The mass balance equation for SiO_2 in one-dimensional flow of water through a porous medium is:

$$\Phi \frac{\partial c}{\partial t} = D_h \frac{\partial^2 c}{\partial x^2} - v \frac{\partial c}{\partial x} + \frac{k_1 \rho_p A'}{C_{eq}}(C_{eq} - C) \qquad (23)$$

where:
- Φ = porosity
- D_h = dispersion coefficient
- v = Darcy velocity
- ρ_p = bulk density of the dry porous medium
- A' = surface area per unit weight of porous medium.

When hot fluids are injected into the formation, the convective SiO_2 transport rate is larger than the dispersive SiO_2 transport rate and as a first approximation, the latter will be neglected. During Run 15004, steam was injected at a temperature of 280°C for a period of 5 days. After a few days, a steady state was established, in which the depleted zone had reached a thickness of approximately 25 cm. In the steady state, $\partial C/\partial t = 0$ and, from (23), equation (24) can be derived:

$$-v(x) \frac{d(C_{eq} - C)}{dx} = k_1 \rho_p A' \frac{(C_{eq} - C)}{C_{eq}} \qquad (24)$$

In the 150 cm simulator, fluids are injected through an injection well in the centre of the vessel. They move outwards and are collected in a perforated circular pipe at a distance of 45 cm from the injection well and are withdrawn from the cell through four production wells that are connected to the circular collector. When water is injected, the Darcy velocity can be calculated from equation (25):

$$v(x) = \frac{I}{2\pi x d \rho_f} \tag{25}$$

where: I = injection rate
x = distance from the injection well
ρ_f = density of the water
d = layer thickness

From (24) and (25):

$$\frac{-d\ (C_{eq} - C)}{(C_{eq} - C)} = \frac{k_1 \rho_p A' 2\pi d \rho_f}{I C_{eq}} \times dx \tag{26}$$

Solution of (26) for the boundary condition $C = 0$ at $x = 0$ yields:

$$-\ln \frac{(C_{eq} - C)}{C_{eq}} = \frac{\pi k_1 \rho_p A' \pi d \rho_f}{I C_{eq}} x^2 \tag{27}$$

In all these derivations it was assumed that $B = 0$ (see equation 16). This assumption is justified since the disturbed surface layer on the quartz grains will have dissolved long before the steady state is reached. The regression equation for the line of best fit through the $\ln k_1 S/V$ data for experiments 3 through 6 is:

$$\ln k_1 S/V = \frac{(-0.72 \pm 0.007)}{T} \times 10^4 + (0.163 \pm 0.014) \times 10^2 \tag{28}$$

so that:

$$\frac{k_1 S}{V} =$$

$$(1.2 \pm 1.7) \times 10^7 \exp [-(7200 \pm 700/T)] \ \mu g \ SiO_2 \ cm^{-3} \ hr^{-1} \quad (29)$$

Expressing r, the solid to liquid ratio, in g dm^{-3},

$$\frac{k_1 S}{V} = \frac{k_1 A' r}{1000} \quad (30)$$

From (29) and (30, using r = 66.7

$$k_1 A' = 1.8 \times 10^8 \exp (-7200/T) \ \mu g \ SiO_2 \ g^{-1} \ hr^{-1} \quad (31)$$

where: T = absolute temperature (K)

assuming that the porous medium consists entirely of quartz (density 2.65 g cm^{-3}) and that $\Phi = 0.35$:

$$\rho_p = (1 - 0.35) \ 2.65 = 1.72 \quad (32)$$

The density of water (at the saturation line) varies with temperature according to (MERCER and PINDER, 1975):

$$\rho_f = 1.27477 - 8.7 \times 10^{-4} T \ g \ cm^{-3} \quad (33)$$

where: T = absolute temperature (K)

The degree of saturation, C/C_{eq}, as a function of x can be calculated from equations (1), (27), (31), (32) and (33).

The SiO_2 dissolution rate, expressed as $\mu g \ SiO_2$/g rock matrix/hour can be calculated from:

$$\frac{\Phi}{2.65\ (1 - \Phi)} \times \left(\frac{\partial C}{\partial t}\right) \text{ dissolution} =$$

$$k_1 A' \ (1 - C/C_{eq}) \qquad (34)$$

where C, t, k_1 and A' are expressed in the appropriate units.

The results of these calculations are shown in Figures 11 and 12. The SiO_2 concentration measured in the production fluid (after steam loss due to flashing) was 523 ppm. When the pressure on saturated water at 280°C is released to the atmosphere, the water separates into steam (38%) and water (62%) so that the SiO_2 concentration at the production well before pressure release was 0.62 x 523 = 324 ppm. For the uppermost curve in Figure 12 at x = 45 cm, C/C_{eq} = 0.996; which corresponds to C = 0.996 x C_{eq} = 0.996 x 520 = 518 ppm. When comparing this to the value that was actually measured, the following facts should be kept in mind:

1. The presence of bitumen lowers the dissolution rate. The effect of bitumen and the lower surface area of the frac sand in the communication path (500 $cm^2\ g^{-1}$) on the dissolution rate were taken into account by using a smaller rate factor. This leads to a calculated concentration of 437 ppm at the production well, still higher than the measured value.

2. The uncertainty in k_1 x A' is quite large (see equation 29).

3. Rather than water, 100% quality steam was injected and the amount of SiO_2 dissolved in the steam can be neglected. Silica dissolution only starts after the steam begins condensing at some distance from the injection well. This effect was simulated by assuming that instantaneous and complete condensation occurs at x_c cm from the injection well. Even though this is an unrealistic assumption, the calculations based on it give a good indication of the direction and order of magnitude of this

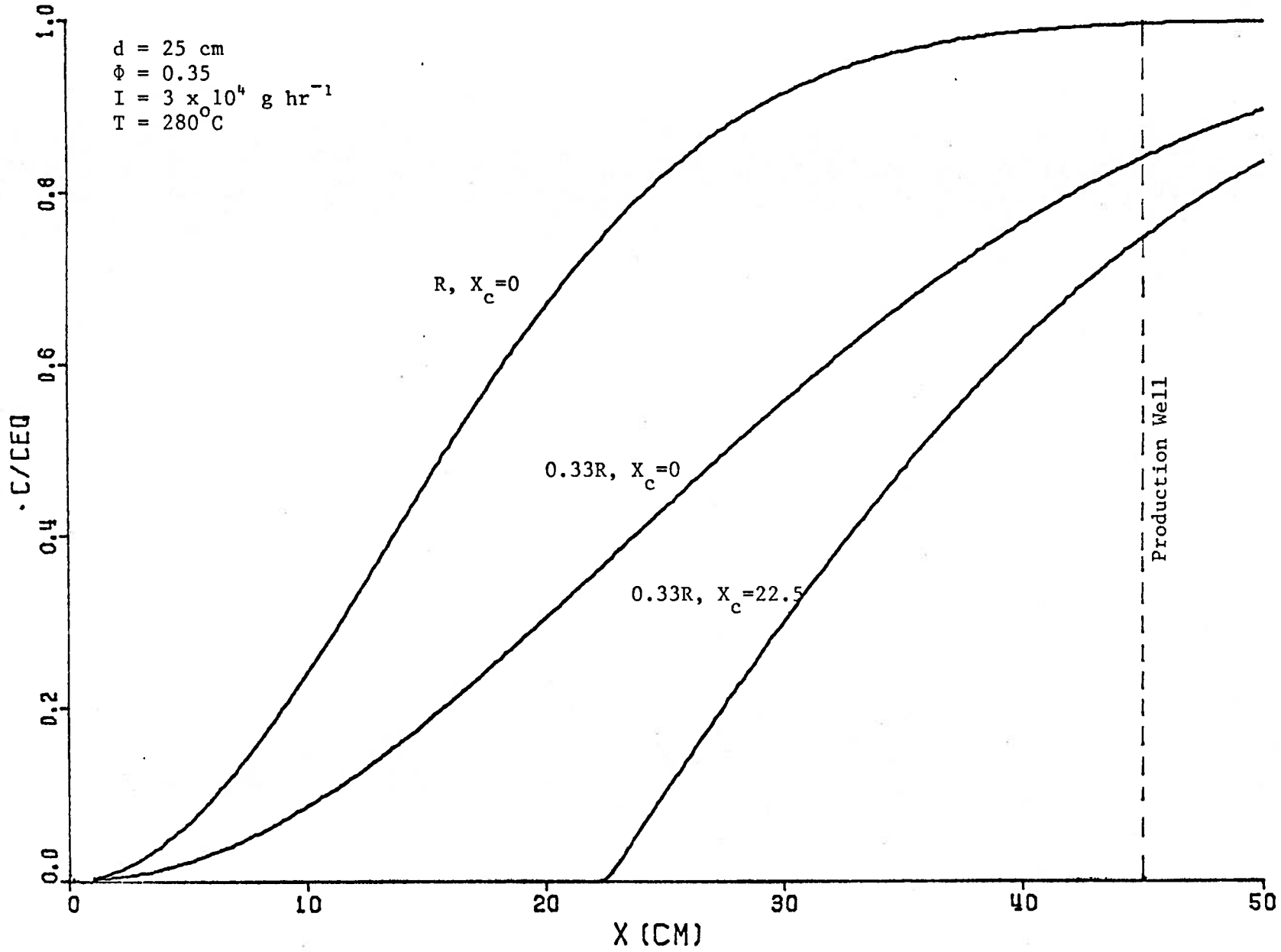

Figure 11. Steady-state quartz saturation in the AOSTRA-ARC 150 cm physical simulator. X = distance from the injection well. R = rate constant according to equation (31). It is assumed that instantaneous and complete condensations of the injected steam take place at X_c cm.

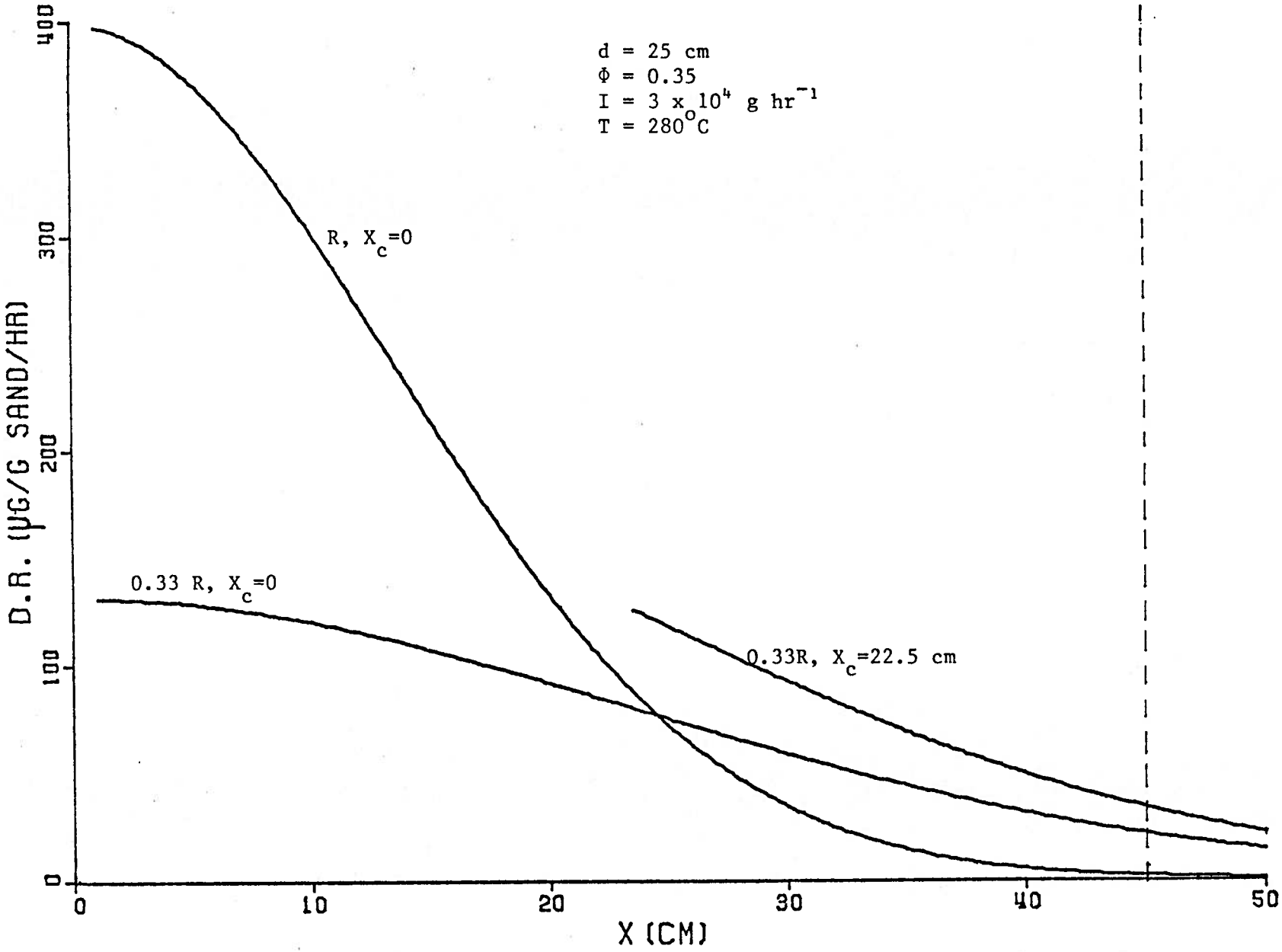

Figure 12. Steady-state quartz dissolution rate in the AOSTRA-ARC 150 cm physical simulator. The symbols used and the assumptions made are the same as those in Figure 11. 1 μg/g sand/hr corresponds to 0.01% of the rock matrix per 100 hours.

effect. They result in a concentration of 388 ppm at the production well.

4. The condensing steam dilutes the solution that is already present. A reliable estimate of the effect of (3) and (4) can only be obtained by numerical methods. In view of the above observations, the measured value is expected to be lower than the calculated value, which is indeed the case.

Dissolution rates in certain zones can be of the order of 100 μg SiO_2/g sand/hr, which is equivalent to 1% of the rock matrix per 100 hours (Figure 12). As dissolution proceeds, the grain size and the surface area of the sand decrease, while the porosity increases. These effects were not taken into account in the calculations described above. It proved impossible to derive an analytical expression that incorporates these factors. Because the sand is unconsolidated, any void spaces that form will likely be filled up by subsidence of the overlying beds unless the sand becomes cemented by asphaltenes. In a field situation, these subsidence effects may be undesirable.

PRECIPITATION OF QUARTZ IN A HYPOTHETICAL FIELD CASE

It was impossible to derive a general rate expression from the precipitation rate experiment, because the results were clearly dependent on the experimental conditions. Also, the induction period cannot be predicted. It was therefore assumed that the rate of concentration change is given by equation (13), regardless of whether the solution is oversaturated or undersaturated with respect to quartz (see also page 9).

Envisage the following, hypothetical situation:

An injection well and a production well are placed 45 m apart in a pay zone of thickness d. Hot water of temperature T_1 is injected in the

injection well. At a distance x_o from the injection well the fluids experience a sudden temperature drop from T_1 to T_2. The latter is a crude way of representing the temperature drop that occurs in the vicinity of the production well. x_o is so large that the aqueous fluids are saturated with respect to quartz at the time they experience the temperature drop. In the steady state, equation (26) is applicable. Now C_{eq} is the equilibrium concentration at temperature T_2. At this point it is convenient to make a coordinate transformation and define y as the distance from the point where the temperature drop occurs, so that:

$$x = y + x_o \tag{35}$$

(24) and (25) now become:

$$-v(y)\ d\ \frac{(C_{eq} - C)}{dy} = k_1 \rho A' \frac{(C_{eq} - C)}{C_{eq}} \tag{36}$$

$$v(y) = \frac{I}{2\pi(y + x_o)\ d\rho_f} \tag{37}$$

From (36) and (37):

$$\frac{-d(C - C_{eq})}{(C - C_{eq})} = E\ (y + x_o)\ dy \tag{38}$$

$$E = \frac{2\pi k_1 \rho_p A' d\rho_f}{I C_{eq}} \tag{39}$$

Solution of (38) for the boundary condition $C = C_o$ at $y = 0$ gives:

$$\ln\left(\frac{C - C_{eq}}{C_0 - C_{eq}}\right) = 1/2\ Ey\ (y + 2\ x_o) \tag{40}$$

C_0 is the equilibrium concentration at temperature T_1, C_{eq} is the equilibrium concentration at temperature T_2.

The quartz precipitation rate, expressed as percent of the rock matrix per 10^4 hours is given by equation (41):

$$\text{precipitation rate} = \frac{\Phi}{2.65\ (1 - \Phi)} \left(\frac{\partial C}{\partial t}\right)_{\text{precipitation}} = k_1 A' \frac{(C - C_{eq})}{C_{eq}} \qquad (41)$$

The degree of saturation of the aqueous fluid and the precipitation rate of quartz as functions of y calculated from equations (31), (32), (33), (39), (40) and (41), are shown in Figure 13 and 14. The case most closely approaching a real field situation is that in which T_1 = 204°C. The injection rate used in the calculation corresponds to approximately 1000 bpd. The assumed thickness of the depleted interval and the interwell distance are also realistic in terms of a field operation. The figures show that precipitation takes place over a relatively short interval and that on the order of 4 to 8% of quartz can be deposited in 10^4 hours (approx. 417 days), a period much shorter than the expected lifetime of most production wells. The precipitation of quartz may lead to a significant permeability reduction but at the present time a quantitative relationship between the amount precipitated and the resulting permeability reduction is not available. CZAJA (1977) found that the permeability of bitumen free oil sand decreased by 50% when she mixed 1% of amorphous silica with the sand. However, precipitation of quartz rather than amorphous silica may produce completely different results.

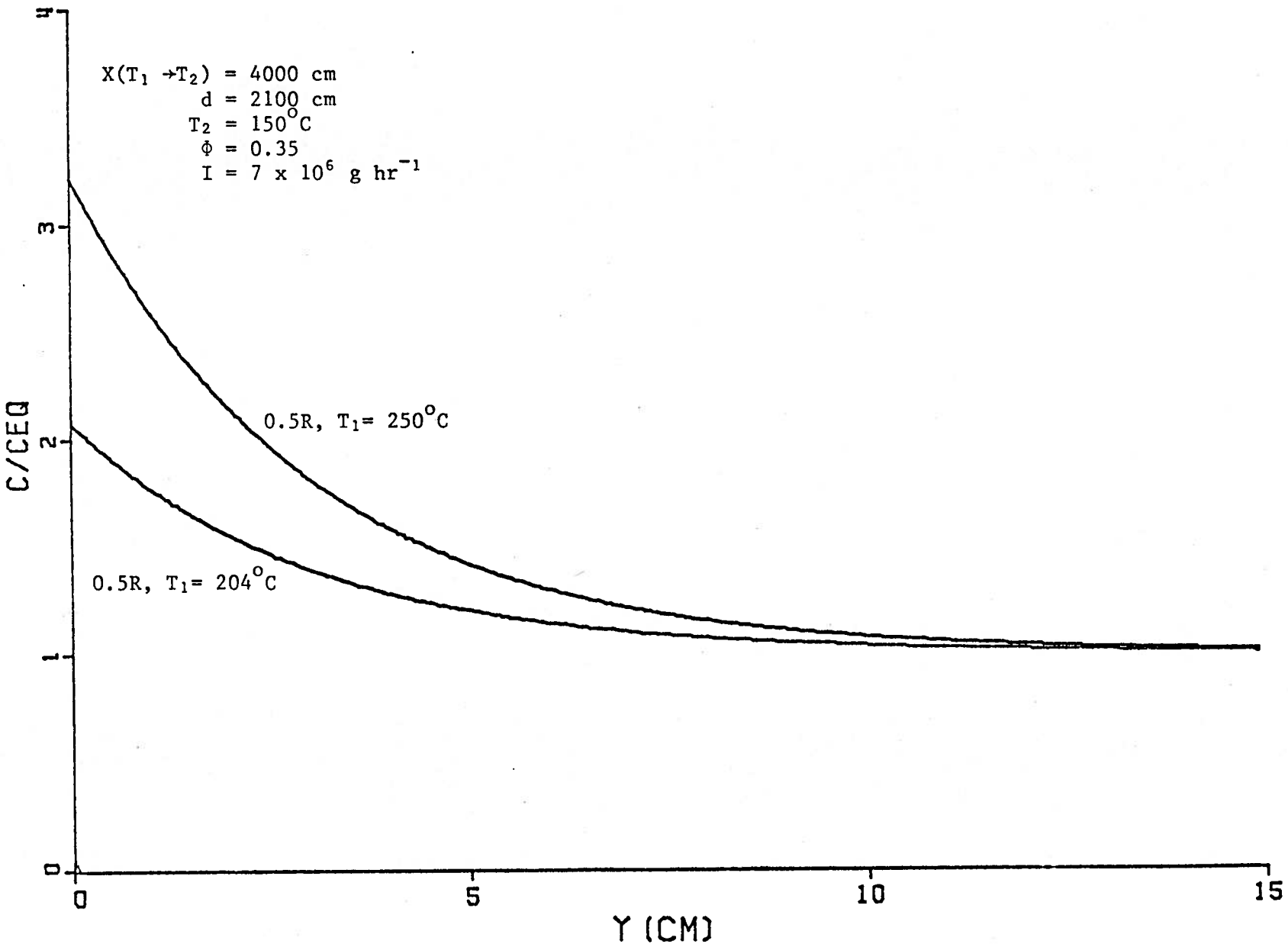

Figure 13. Steady-state quartz saturation as a function if distance from the point where a temperature drop $T_1 \rightarrow T_2$ takes place in a hypothetical field case. X = distance from the injection well to that point. Hot water flow. R = rate constant given by equation (31).

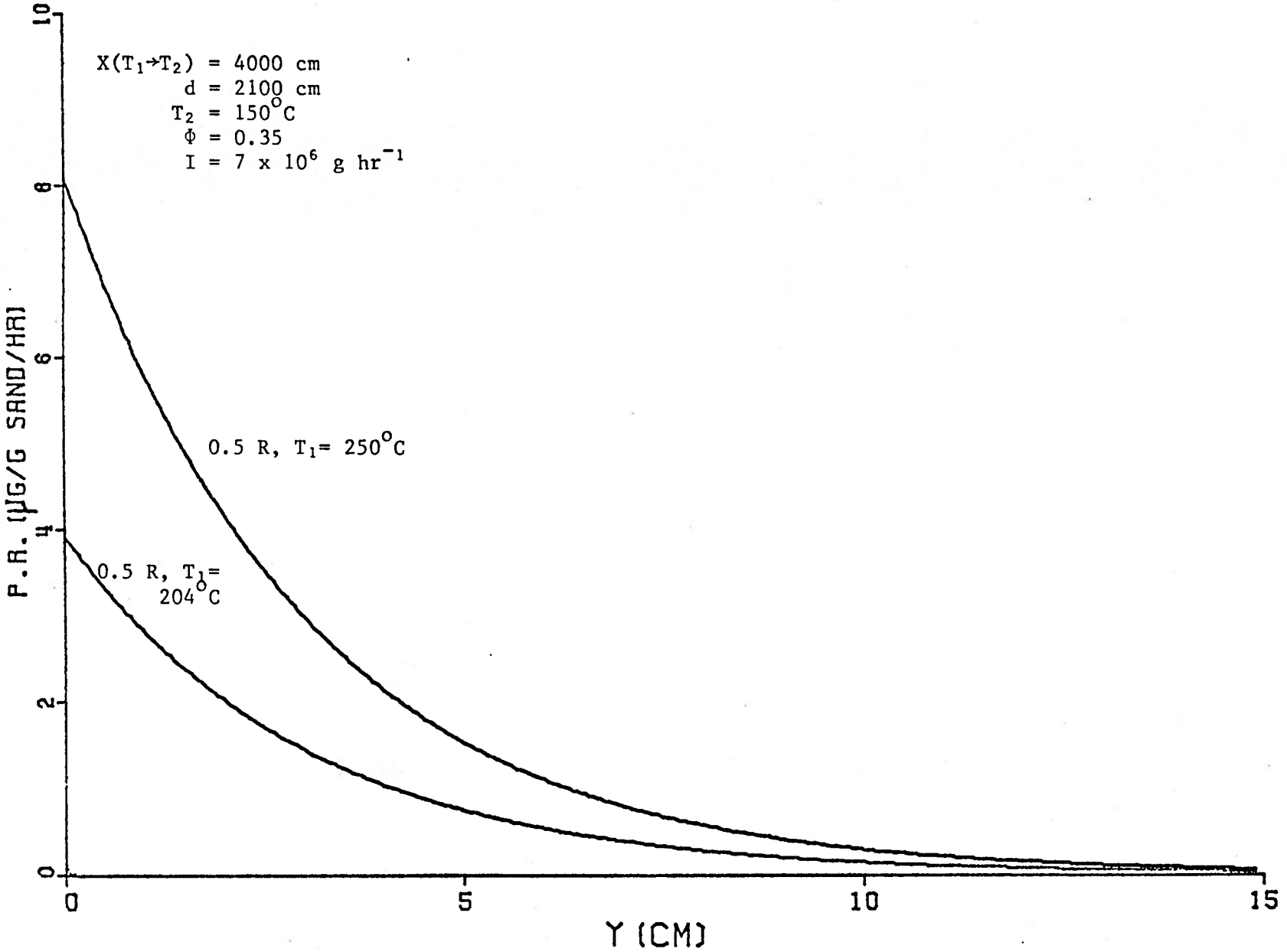

Figure 14. Quartz precipitation rate in a hypothetical field case. The symbols used and the assumptions made are the same as those in Figure 13. 1 µg/g sand/hr corresponds to 1% of the rock matrix per 10,000 hours (=417 days).

FUTURE PLANS

- Develop a mathematical model to describe the behaviour of silica during steam injection.

- Carry out dissolution and precipitation experiments in a flow system. A few of the advantages of this approach are:

  1. The experimental set-up strongly influenced the results of the precipitation experiments and of the dissolution experiments at high pH. In a flow system the experimental conditions are much closer to those encountered in the field and can, therefore, be more easily extrapolated to a field situation.

  2. Precipitation experiments in a flow system will enable the establishment of a quantitative relation between permeability reduction and the amount of SiO_2 that is precipitated.

  3. The effect of hydrodynamic dispersion, that was neglected in the steady state calculations, can be studied in more detail.

  4. The results of flow experiments can be compared to those obtained from a mathematical model and can be used to refine the model.

ACKNOWLEDGEMENTS

Most of the experimental work was carried out by Mr. L.R. Holloway. The surface areas of the sand samples were measured by Mr. A. Mo, Western Regional Laboratory, Federal Department of Energy, Mines and Resources. The manuscript was typed by T. Ranch and L. Harder, who also assisted in the lay-out.

REFERENCES

ALEXANDER G.B. (1954) The polymerization of monosilicic acid. *J. Amer. Chem. Soc.* 76, 2094-2096.

BAYLISS P. and LEVINSON A.A. (1971) Low temperature hydrothermal synthesis from dolomite or calcite, quartz and kaolinite, *J. Appl. Chem.* 19, 109-114.

BERGMAN I. (1963) Silica powders of respirable size. III Dialysis of quartz powders against dilute sodium hydroxide. *J. Appl. Chem.* 13, 319-323.

BOON J.A. (1977a) Fluid-rock interactions during steam injection: *The Oil Sands of Canada-Venezuela, CIM special volume* 17, 133-138.

BOON J.A. (1977b) Mass transfer of silica during steam injection. *Proc. 2nd Int. Symp. Water-Rock Interaction.* Strasbourg, France, August 17-25, IV_{199}-IV_{206}.

CECIL C.B. and HEALD C.T., (1971) Experimental investigation of the effects of grain coatings on quartz growth. *J. Sed. Petr.* 41, 582-584.

COURNOYER R.A., KRANICH W.L. and SAND L.B. (1975) Zeolite crystallization kinetics related to dissolution rates of quartz reactant. *J. Phys. Chem.* 79, 1578-1581.

CRERAR D.A. and ANDERSON G.M. (1971) Solubility and solvation reactions of quartz in dilute hydrothermal solutions. *Chem. Geol.* 8, 107-122.

CZAJA I. (1977) *OSRC Report,* November 1977, 19 pp.

DOREMUS R.H. and ALIM-MARVASTI F. (1973) The rate of dissolution of amorphous silica in water. *NTIS Report AD*, 762-767.

ERNST W.G. and BLATT H. (1964) Experimental study of quartz overgrowths and synthetic quartzites. *J. Geol.* 72, 461-470.

FRIEDMAN G.M., ALI S.A. and KRINSLEY D.H. (1976) Dissolution of quartz accompanying carbonate precipitation and cementation in reefs: example from the Red Sea. *Jour. Sed. Petrol.* 46, 970-973.

GOTO K. (1956) Effect of pH on polymerization of silicic acid. *J. Phys. Chem.* 60, 1007-1008.

HARVEY W.W., MAKRIDES A.C., SLAUGHTER J. and TURNER M.J. (1976) Kinetics of silica condensation in brines. *ERDA Report COO*-2607-4, 25-35.

HEALD M.T. and RENTON J.J. (1966) Experimental study of sandstone cementation. *J. Sed. Petrol.* 36, 977-991.

HENDERSON J.H., SYERS J.K. and JACKSON M.L. (1970) Quartz dissolution as influenced by pH and the presence of a disturbed surface layer. *Israel J. Chem.* 8, 357-372.

KITAHARA S. (1960) The polymerization of silicic acid obtained by the hydrothermal treatment of quartz and the solubility of amorphous silica. *Rev. Phys. Chem. Japan* 30, 131-317.

MAXWELL J.C. (1960) Experiments on compaction and cementation of sand: *Rock Deformation, Geol. Soc. Amer. Memoir* 79, 105-132 Ed. D. Griggs and J. Handin.

MERCER W.J. and PINDER G.F. (1975) Hot water geothermal simulation model using finite element method. *USGS Report*, 75-574.

MOORE G.S.M. and ROSE H.E. (1975) Dissolution of powdered quartz. *Nature* (London) 253, 525-527.

OWEN L.B. (1975) Precipitation of amorphous silica from high-temperature hypersaline geothermal brines. *NTIS Doc.* UCRL 51866.

PARAGUASSA A.B. (1972) Experimental silicification of sandstone. *Geol. Soc. Amer. Bull.* 83, 2853-2858.

PETTIJOHN F.J., POTTER P.E. and SIEVER R. (1972) Sand and sandstone. *Springer Verlag, New York* 618 pp.

REDFORD D.A. and COTSWORTH P.F. (1974) In-situ production problems. Eng. *Inst. Canada, Tar Sands Conf. Edmonton,* April 17-19, 1974, 359-369.

RIMSTIDT J.D. and BARNES H.L. (1977) Kinetic evaluation of the quartz geothermometer. *Abstr. Ann. Meeting Geol. Soc. Amer.*, Seattle, U.S.A. November, 1142.

SEWARD T.M. (1974) Determination of the first ionization constant of silicic acid from quartz solubility in borate buffer solutions to 350°C. *Geochim. Cosmochim. Acta* 38, 1651-1664.

SPRUNT E.S. and NUR A. (1976) Reduction of porosity by pressure solution: *Experimental Verification, Geology* 4, 463-466.

VAN LIER J.A., DE BRUYN P.L. and OVERBEEK J.Th.G. (1960) The solubility of quartz. *J. Phys. Chem.* 64, 1675-1682.

WALTHER J.V. and HELGESON H.C. (1977) Calculation of the thermodynamic properties of aqueous silica and the solubility of quartz and its polymorphs at high pressures and temperatures. *Amer. J. Sci.* 277, 1315-1351.

APPENDIX

The Effect of Withdrawing Consecutive Samples on the Measured Rate Constants.

In order to be able to use the autoclaves efficiently and to obtain rate constants within a reasonable period of time, it was necessary to withdraw consecutive samples from one autoclave. This leads to an increase in the value of S/V after each sampling. As samples were small, it was thought that the final results would not be affected to a large extent. Very recently, a fitting procedure that takes the change in S/V into account was brought to our attention. Equation (14) can be written as:

$$-\ln \frac{C_{eq} - C_i}{C_{eq} - C_{i-1}} = \frac{k_1 S}{C_{eq}} \times \frac{\Delta t_i}{V_i} \qquad (a)$$

where: $C_i = C_{SiO_2}$ at $t = t_i$

$C_{i-1} = C_{SiO_2}$ at $t = t_{i-1}$

$\Delta t_i = t_i - t_{i-1}$

V_i = volume of the aqueous phase between sampling times t_{i-1} and t_i

Now $\frac{\Delta t_i}{V_i}$ can be plotted against $-\ln \frac{(C_{eq} - C_i)}{(C_{eq} - C_{i-1})}$ and $k_1 S$ can be calculated from the slope of the least squares regression line through the data points. Because the quotient $(C_{eq} - C_i)/(C_{eq} - C_{i-1})$ contains two measured concentrations, both of which are subject to experimental error, the standard deviation in the quotient tends to be quite large. Also, the errors in consecutive data points are not independent. As a result, the $k_1 S$ values that are obtained by the least squares regression method described on page 17 have a large standard deviation. The experimental data were treated as outlined above. Only for experiments 7, 19 and 21 was there a statistically

significant difference between the results thus obtained and those presented in Table 3. The revised values that are given in Table A-1 are in better agreement with the general results that were obtained in other experiments that were carried out under similar conditions. The revised value of the activation energy for dissolution calculated from experiments 19 and 21 is 26.8 ± 4.0 kcal $mole^{-1}$, which is not significantly different from that given in Table 4. The revised values of Δ(bit) in Table 5 are 0.38 ± 0.45 for experiment pair 19 and 28 and 0.44 ± 0.30 for experiment pair 21 and 30. The large standard deviation illustrates the point that was made earlier. The general conclusions that were drawn in this report are not altered by the modified data treatment procedure. However, final conclusions will only be drawn after the problem posed by the fact that the errors of consecutive data point pairs are not independent has been solved.

Table A-1. Revised dissolution rate constants. For legend see Table 3. SC indicates that the change in S/V caused by withdrawing consecutive samples has been taken into account.

	EXPERIMENT						CLQ	E SQ	D	DD	B	DB	KSE-3	DKSE-3	LNKS	DLN	CO	DCO
7	CL. S. DETON. H2O	20	G/L	250C.	SFPE	SC	415.4	0.07	34.50	11.60	0.052	0.075	14.33	4.82	9.57	0.34	-7.4	23.1
19	CL. S. 0.01M BORAX	20	G/L	200C.		SC	467.6	0.41	3.57	1.38	0.122	0.079	1.67	0.65	7.42	0.39	109.5	12.7
21	CL. S. 0.01M BORAX	20	G/L	250C.		SC	764.7	2.71	32.94	3.41	0.075	0.024	25.19	2.61	10.13	0.10	70.7	13.4